

FACILITY FORM 602

N 66-10888

(ACCESSION NUMBER)

(THRU)

(PAGES)

(CODE)

(NASA CR OR TMX OR AD NUMBER)

(CATEGORY)

PURDUE UNIVERSITY



GPO PRICE \$ _____

CFSTI PRICE(S) \$ _____

Hard copy (HC) 3.00

Microfiche (MF) .75

ff 653 July 65

SCHOOL OF AERONAUTICAL AND ENGINEERING SCIENCES

QUARTERLY PROGRESS REPORT

STUDY OF RECIRCULATING GAS FLOW FIELDS IN
THE BASE REGION OF SATURN-CLASS VEHICLES

NASA Contract No. NAS 8-11485

May 1 - July 31, 1965

Lafayette, Indiana

QUARTERLY PROGRESS REPORT

Study of Recirculating Gas Flow Fields in
the Base Region of Saturn-Class Vehicles

NASA Contract No. NAS 8-11485

submitted to

National Aeronautics and Space Administration
George C. Marshall Space Flight Center
Huntsville, Alabama
Attention: FR-EC

prepared by

School of Aeronautics, Astronautics and Engineering Sciences
Purdue University
Lafayette, Indiana

Principal Investigator: Professor Richard F. Hoglund

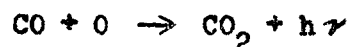
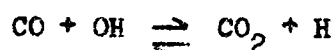
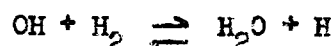
Reporting period: May 1 - July 31, 1965

Table of Contents

	Page
Abstract	ii
1. Introduction	1
2. Chemical Reactions in the Air-Combustion Product Mixing Layer	3
3. Study of Calculation Techniques for the Non-Equilibrium Boundary Layer and Free Shear Layer	18
4. Possible Effects of Reactions on Turbulent Mixing Processes	26
5. Future Work	45
6. Personnel	46
References	47
Appendix	
A Discussion of Reactions System	52
B Reaction Rates	56
C Reaction Energies	66
D Discussion of the Carbon Monoxide - Oxygen Reaction	67
E Transformation of the Compressible Mixing Layer	72

Abstract

The relative rates and energy release of various reactions in the exhaust plume - air mixing layer are examined in an approximate fashion. It is found that the most important reactions are, in decreasing order,



Since all of these are two-body reactions, it is concluded that binary scaling should be applicable to the afterburning plume. Since all of these reactions involve intermediate species, "flame front" approximations are not useful in scaling reaction effects. The third listed reaction may account for some of the observed radiation from afterburning plumes. Various numerical methods for solution of the equations which describe a non-equilibrium, non-similar boundary layer or mixing layer were investigated. It was concluded that an implicit integration scheme offered significant advantages; the main problem in such a program would be the determination of species concentrations when some reactions are close to equilibrium. Subsequently, reports were received from other NASA contractors which indicated that the procedure which we would recommend was already being pursued. The mathematical transformation of a high speed reacting mixing layer to an equivalent low speed mixing layer is examined. It is concluded that the Coles-Crocco transformation, which has been very useful in the treatment of high speed boundary layers, is

not directly useful when applied to mixing layers. Further work on this subject is indicated. The possible effects of chemical reactions on turbulent transport are discussed. It is shown that non-equilibrium reactions, when internal states are accounted for, contribute to the vorticity. Also, the density changes associated with chemical reactions add a new term into the momentum transport equation. Thus, reactions are expected to have a definite effect on turbulent transport processes.

1. Introduction

This report nominally covers the period of May 1 - July 31, 1965. Due to a misunderstanding of report requirements, monthly reports were submitted at the beginning of this project. The current report is the first one submitted on a quarterly basis; for completeness and to avoid confusion, the report will cover all work accomplished through July on this program without reference to the preceding reports.

The project reported on herein is a study of certain chemical and chemical-radiative effects on the base flow field associated with multiple-nozzled launch vehicles of the Saturn-type. The level of effort consists of three graduate students employed on a half-time research basis. Particular subjects under investigation are: 1) delineation of the controlling and energetically most important reactions which occur in the air-combustion product mixing layer to determine the applicable chemical scaling laws; 2) evaluation of various analytical techniques for calculation of the non-similar boundary layer and free shear layer involving finite-rate chemical reactions; and 3) preliminary evaluation of the nature of the effect of energetic chemical reactions on the turbulent stream mixing process. The investigators are, respectively, Messrs. H.F. Nelson, E.C. Palmreuter and J.P. Nuyts.

In addition to the above studies, substantial effort in early stages of the project was spent in familiarization with the general base heating problem and with the work of the other NASA contractors in this area.

This effort was expended to provide a background which, hopefully, will ensure the aiming of specific research efforts in a direction that will be useful to the overall NASA program. Such efforts, of course, are not reported on here.

2. Chemical Reactions in the Air-Combustion Product Mixing Layer

It is expected that most low altitude plume phenomena associated with air-combustion product chemical reactions will be characterized by short reaction times compared with the appropriate fluid mechanic times. That is, the rate of progress of the chemical reactions will be limited by the rate of supply of reactants via fluid mechanical diffusion processes (in most cases turbulent) rather than by the rates of the governing chemical reactions themselves. If this were always the case scaling could be accomplished by the well developed fluid mechanical scaling laws alone, without consideration of the chemical reactions.

However, when simulation on a sufficiently small scale or of a sufficiently high altitude condition is attempted, the fluid mechanic times and the chemical reaction times can become of the same order. To determine when this situation arises we have to decide which of the chemical reactions are rate controlling and energetically important. If the critical reactions are found to be of the two-body type (or if the importance of three-body reactions is negligible) the concept of binary scaling¹⁹ can be used. Binary scaling is achieved if the product ρL is maintained constant, where ρ is the fluid density and L is the appropriate dimension of the model or vehicle.

Some insight into which reactions are important could be obtained from examination of an appropriate chemical equilibrium solution to the combustion product - air mixing layer. The rates of chemical specie production required to maintain the equilibrium condition could give an

inexact indication of which reactions are important provided that the reaction paths are properly identified. This, of course, is not always possible without previous experience in the same problem. A more serious limitation to our pursuit of this path, however, is that no equilibrium solutions to the mixing layer seem to have been accomplished. Hence, it is recommended that those NASA contractors currently engaged in performing mixing layer analyses (either by the matched inviscid flow-free shear layer technique or by the "entire jet" calculation) combine their programs with a chemical equilibrium thermochemical program to generate equilibrium species profiles. As will be shown below the "flame front" calculations are an inadequate substitute since they fail to reveal the concentrations of the reaction-controlling intermediate species.

Lacking either equilibrium species profiles or complete finite rate calculations, we have employed some approximations in the reaction chemistry to enable us to calculate rough intermediate species profiles and thus provide at least a general idea of which reactions are important and how they should be scaled in model testing.

To arrive at a manageable system of reactions we deleted certain reactions from an original set of 21 reactions involving 11 different chemical species. The reactions which were dropped along with the reasons are listed in Appendix A.

The reaction system which was employed considered 11 chemical reactions believed to be possible in the exhaust plume of a rocket engine burning RP-1 and liquid oxygen.

Table I

$H + OH + M$	\rightleftharpoons	$H_2O + M$	1
$H + H + M$	\rightleftharpoons	$H_2 + M$	2
$O + O + M$	\rightleftharpoons	$O_2 + M$	3
$H + O + M$	\rightleftharpoons	$OH + M$	4
$CO_2 + M$	\rightleftharpoons	$CO + O + M$	5
$OH + OH$	\rightleftharpoons	$H_2O + O$	6
$CO + OH$	\rightleftharpoons	$CO_2 + H$	7
$OH + H_2$	\rightleftharpoons	$H_2O + H$	8
$H + O_2$	\rightleftharpoons	$OH + O$	9
$O + H_2$	\rightleftharpoons	$OH + H$	10
$CO + O$	\rightleftharpoons	$CO_2 + h\nu$	11

where M is any specie.

Borrowing an idea from the work of Kaskan^{9,10}, by assuming reactions 1, 3, 4 were in equilibrium and by using an appropriate species diffusion profiles the concentrations of OH, H, and O could be calculated. We will discuss briefly the choice of species profile.

Two basic approaches to the development of chemical species profiles have been developed. These are 1) the "entire jet" approach and 2) the inviscid flow - mixing layer approach.

The entire jet approach neglects the presence of shock structure and assumes that the boundary layer assumptions apply throughout the exhaust plume. Feigenbutz⁵ and Rozsa⁴ have used this approach.

The mixing-layer approach assumes that a method of characteristics solution is correct for the inviscid inner core of the exhaust plume and for the external flow. The boundary layer type equations are used for the viscous flow external to the inner inviscid core, with boundary conditions on the boundary between the inner and outer parts defined by the method of characteristics inviscid solution. Vasiliu⁶ and Feigenbutz⁷ have used this approach.

There are advantages and disadvantages to both methods. The entire jet method is simplest, but its use is restricted to low altitude, near balanced plumes⁴. The mixing layer method is good at any altitude where conditions for inviscid flow exist. Both methods are limited since the accuracy of the turbulent transport coefficients is not very good.

Feigenbutz and Rozsa both used a reaction approximation called the "flame front" concept. The flame front is assumed to be a position between a fuel-rich stream and an oxidant-rich stream where combustion is complete. On the fuel-rich side of the flame front, no oxygen is present, and on the other side of the flame front no fuel is present. The fuel and oxygen species diffuse toward each other with complete combustion occurring very rapidly at the flame front.

The flame front concept does not allow any intermediates such as OH, H, O; from Kaskan⁹,

$$[\text{OH}] = \sqrt{K_9 K_{10} [\text{O}_2] [\text{H}_2]} \quad (K_9, K_{10} \text{ are equilibrium constants})$$

and either $[\text{O}_2]$ or $[\text{H}_2]$ is zero throughout the whole plume in the

"flame front" model. Thus, flame front profiles could not be used; in the absence of better information the frozen species concentration profiles of Rozsa¹¹ were used for our calculations (Figures 2 and 3).

Assuming the three-body reactions (1,3,4) to be in equilibrium would seem to imply that binary scaling does not hold. However, if it can be shown that the energy associated with these three-body reactions is unimportant in this calculation it implies that they will be unimportant in the actual situation. The maximum energy release occurs on recombination and assuming the three-body reactions to be in equilibrium is allowing a much higher rate of recombination than binary scaling would allow. The concentrations of O, OH, and H found this way should represent a lower limit.

From the three-body reactions named above the following expressions for the concentrations of H, OH, and O were obtained as follows:

$$[O] = \sqrt{[O_2]/K_3}$$

$$[H] = \sqrt{[H_2O] / ([O] (K_4) (K_1))}$$

$$[OH] = [H] [O] K_4$$

For a graph of the concentrations so calculated, see Figure 1.

A review of literature for reaction rates for each of the 11 reactions was done. As can be seen from the results (listed in Appendix B) some of the rates are not too well agreed upon as of yet.

The forward and reverse reaction rates were calculated in $\frac{\text{gr-mole}}{\text{cm}^3 \text{ sec}}$. The forward rate was calculated by multiplying the concentrations

of the reactants by the rate constant. The forward rate constants used are the starred ones in Appendix B. The reverse rate was calculated by multiplying concentrations of the products by the reverse rate constant. The reverse rate constant was assumed to be the forward rate constant divided by the equilibrium constant.

The enthalpy of each reaction was found by subtracting the reverse rate from the forward rate and multiplying by the enthalpy of the reaction at the specific temperature. Appendix C gives the values across the exhaust at $x^* = 17.4$ x^* , the non-dimensional axial distance, is the distance behind the nozzle exit divided by the radius of the exhaust nozzle exit.

Table II shows in order of decreasing enthalpy the number of the most energetic chemical reactions as a function of the non-dimensional radius r^* and the temperature. r^* is equal to the radius of the point of interest divided by the radius of the exhaust nozzle exit. The temperature is in degrees Kelvin. The data for the concentrations was taken from Rozsa¹¹ for a balanced pressure exhaust.

Table III shows the chemical reactions in which the forward reaction rate is greater than $.001 \frac{\text{gr-mole}}{\text{cm}^3 \text{ sec}}$ at $x^* = 17.4$ as a function of r^* .

Table IV shows the chemical reactions in which the reverse reaction rate is greater than $.001 \frac{\text{gr-mole}}{\text{cm}^3 \text{ sec}}$ at $x^* = 17.4$ as a function of r^* .

The temperature given in each table is the temperature profile as a function of r^* at $x^* = 17.4$. It must be remembered that the temperature is a function of the various concentrations across the exhaust.

Table II Reactions in which the energy release is more
than $1 \text{ cal}/(\text{cm}^3 \text{ sec})$ at $x^* = 17.4$

radius (r^*)	decreasing energy →	Temp. ($^{\circ}\text{K}$)
.3	8, 7, 11	1438
.4	8, 7, 11, 10^{R} †	1497
.5	8, 7, 11, 10^{R}	1511
.6	8, 7, 11, 10^{R}	1539
.7	8, 7, 11, 10^{R}	1567
.8	8, 7, 11, 10^{R}	1595
.9	8, 7, 11, 10^{R}	1595
1.0	8, 7, 11, 10^{R}	1581
1.1	8, 7, 11, 10^{R}	1539
1.2	8, 7, 11, 10^{R}	1469
1.3	8, 7, 11	1400
1.4	8, 7	1302
1.5	8	1190
1.6	8	1078
1.7		938
1.8		812

† the superscript R stands for the reverse of the reaction listed in Table I

Table III Forward reaction rates greater than

$.001 \frac{\text{gr-mole}}{\text{cm}^3 \text{ sec}}$ at $x^* = 17.4$

radius (r^*)	decreasing rate —————→	Temp. ($^{\circ}\text{K}$)
.3	8, 7, 6	1483
.4	8, 7, 6	1497
.5	8, 7, 6	1511
.6	8, 7, 6, 10	1539
.7	8, 6, 7, 10, 9	1567
.8	8, 6, 7, 9, 10	1595
.9	8, 6, 7, 9, 10	1595
1.0	8, 6, 7, 9, 10	1581
1.1	8, 6, 7, 10, 9	1539
1.2	8, 6, 7	1469
1.3	8	1400
1.4	8	1302
1.5	8	1190
1.6		1078
1.7		938
1.8		812

Table IV Reverse reaction rates greater than

$$1001 \frac{\text{Mg-Atile}}{\text{cm}^3 \text{ sec}} \text{ at } r^* = 17.6$$

radius (r^*)	decreasing rate —————→	Temp. ($^{\circ}\text{K}$)
.3	8, 6	1443
.4	8, 6	1497
.5	8, 6	1511
.6	6, 8	1539
.7	6, 8, 9	1567
.8	8, 6, 9	1595
.9	8, 6, 9	1595
1.0	6, 8, 9	1581
1.1	6, 8, 9	1539
1.2	6	1469
1.3		1400

Use of the frozen profiles obviously causes an underestimation of the temperatures in the reaction zone. Until equilibrium profiles are generated, however, there seems to be no other reasonable alternative.

To further check the applicability of binary scaling the energy release associated with the three-body reactions must be evaluated. If binary scaling is possible this energy of recombination must be much less than that of the two-body reactions.

To get an upper limit on the recombination energy, it should be possible to multiply the maximum concentration of the recombining species times the enthalpy at that temperature. This essentially says

that all the recombining species recombine and give an upper limit on the energy.

The maximum intermediate concentrations are

$$[OH]_{\max} = 2.478 \times 10^{-8} \frac{\text{gr-mole}}{\text{cm}^3}$$

$$[H]_{\max} = 7.083 \times 10^{-9} \frac{\text{gr-mole}}{\text{cm}^3}$$

$$[O]_{\max} = 8.251 \times 10^{-9} \frac{\text{gr-mole}}{\text{cm}^3}$$

In each case the intermediate which gives the maximum energy was used. The energies are given in Table V.

To get the energies into units to compare with the two-body energies, one must multiply by the appropriate transport velocity and divide by the diffused distance. But this is the same time as the ratio of the axial velocity to axial distance.

From Rozsa¹¹ the velocity at $x^* = 17.4$ is 5270 ft/sec. The distance $x = (17.4)r$ ft. where r is the nozzle exit radius in feet.

The energy calculation (Table V) shows, for a nozzle exit radius of one foot, that the three-body recombination energy is a factor of 10^7 less than the most energetic two-body reaction and a factor of 100 less than the energy of the reactions considered in Table I. This indicates that the three-body reactions are not important and that binary scaling seems to be a good assumption.

Table V Three-body recombination energy as a function of the nozzle exit radius r (in feet) - negative sign means energy release

Reaction Number	H <u>kilo-cal</u> <u>gr-mole</u>	Intermediate	Energy <u>kilo-cal</u> <u>cm³</u>	Energy <u>kilo-cal</u> <u>cm³ sec</u>
1	- 122.4	OH	- 3.0×10^{-6}	- $9.03 \times 10^{-5}/r$
3	- 121.5	O	- 1.0×10^{-6}	- $3.01 \times 10^{-5}/r$
4	- 105.5	H	- 7.5×10^{-7}	- $2.25 \times 10^{-5}/r$

The above rough analysis shows that reactions 8 and 7 are the dominant ones in the burning of the turbulent exhaust gases of a rocket.



These two reactions both involve the intermediates OH and H; one involves H_2 and one CO, the two combustibles from the nozzle exhaust.

It was shown that the energy release of the three-body recombination reactions was much smaller than the energy release of the two-body reactions 8 and 7. This rough estimate implies that in the non-equilibrium turbulent exhaust, binary scaling will be a good assumption. In assessing the onset of non-equilibrium effects, the

intermediate species OH and H must be considered as they are participants in the most important reactions.

It may be noted from Appendix C that reaction 11, the radiation-releasing CO-O reaction, is third in energetic importance among the reactions considered. The radiation released is about $\frac{1}{2}\%$ of the total energy released in the mixing layer; thus, we should examine this reaction more closely when considering the radiative properties of the plumes.

The radiation from the CO-O reaction apparently is near-continuous in nature. It extends from about 3000 Å to 6500 Å with a center at about 4200 Å. At high temperatures, there appears to be strengthening of the ultra-violet end of the spectrum¹⁶. Because of the interest in the radiation from plumes of the type considered here, the CO-O reaction system is discussed in Appendix D.

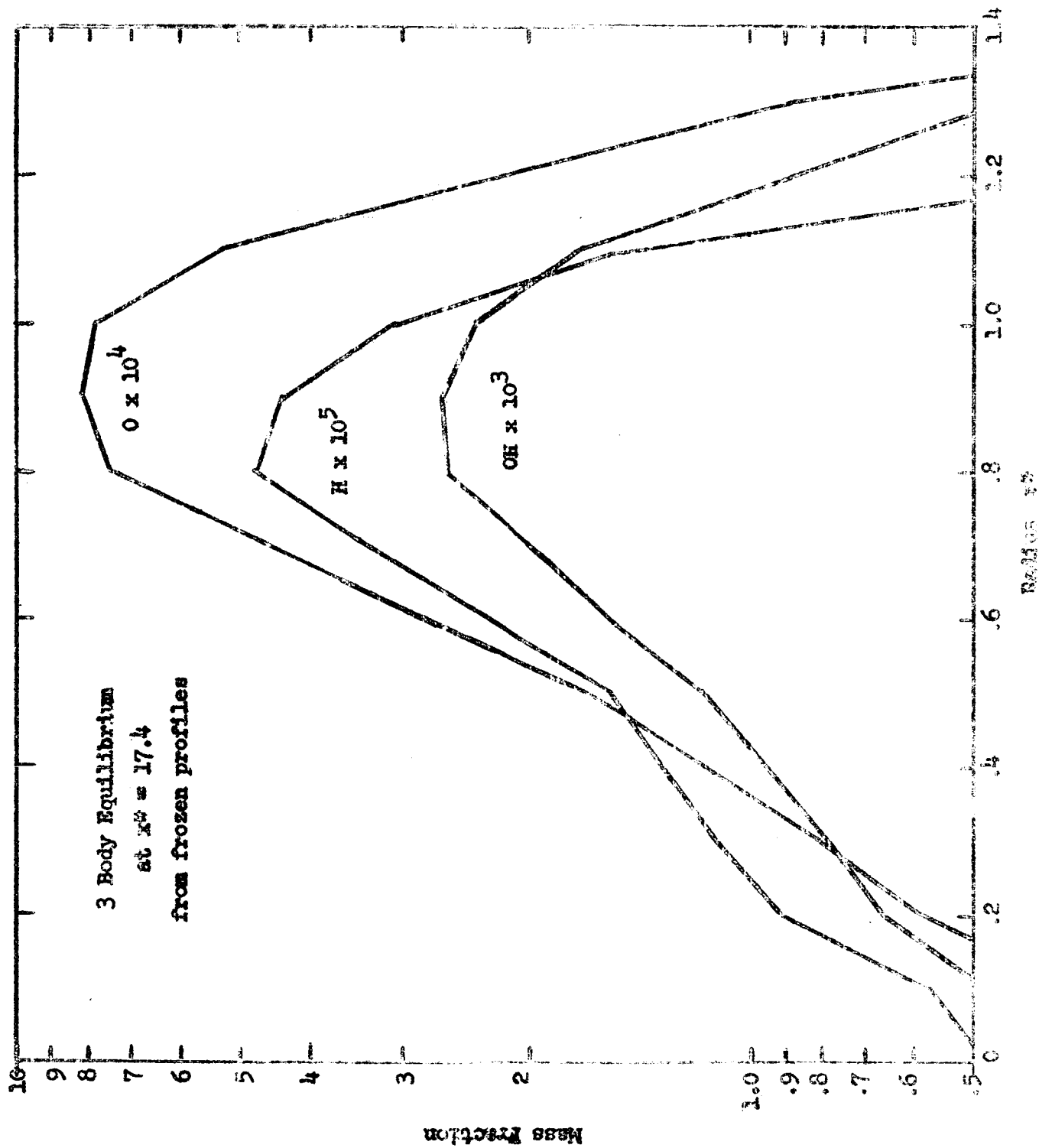


FIGURE 1. EQUILIBRIUM PROFILE CALCULATIONS

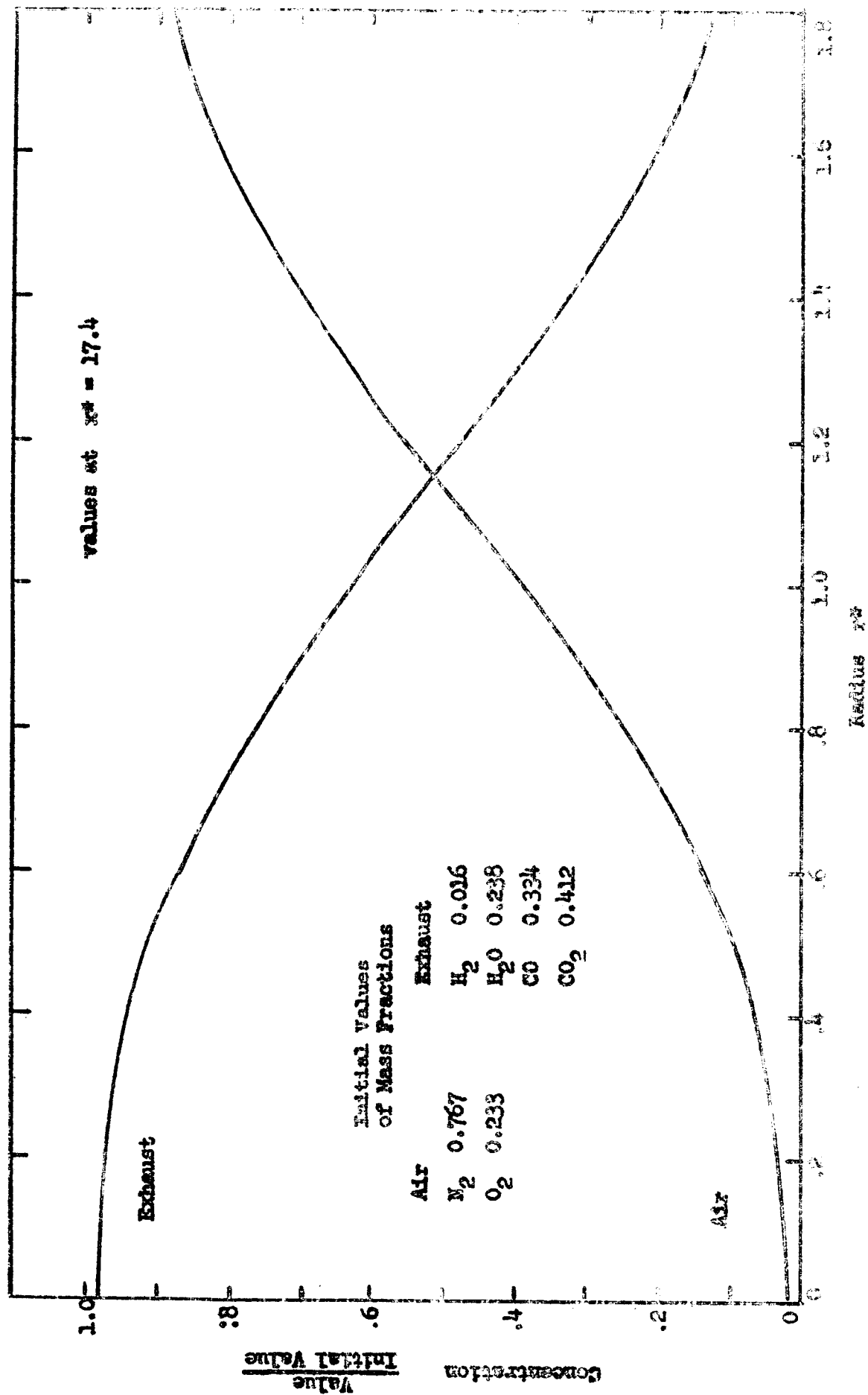


Figure II Proton Specie Concentrations (from Rosen, Ref. 11)

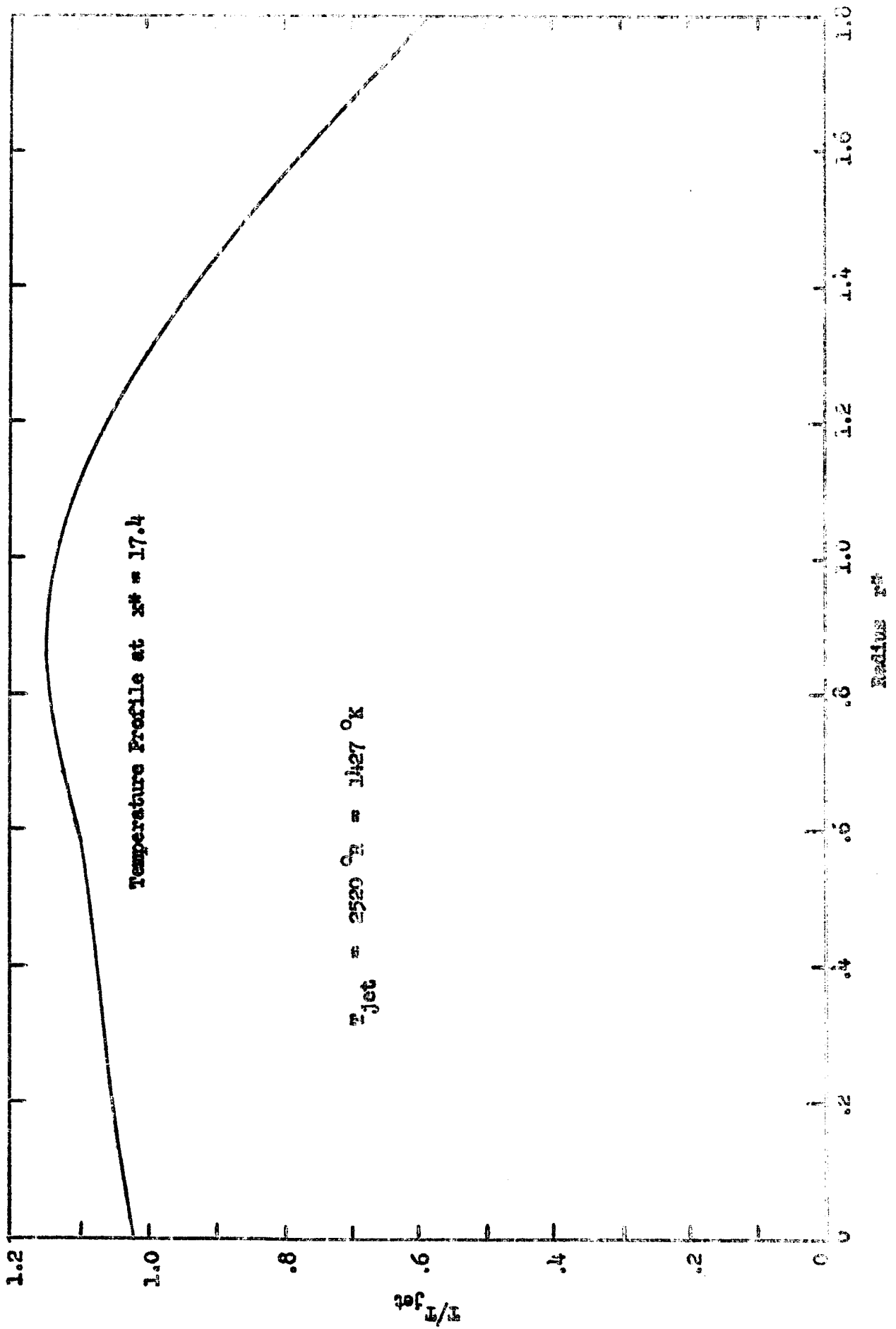


Figure III Frozen Temperature Profile (from Hossa, Ref. 11)

3. Study of Calculation Techniques for the Non-Equilibrium Boundary Layer and Free Shear Layer

The object of this study was to find the "best" available nonsimilar solution to the chemically reactive boundary or shear layer. After a search of the current literature, it was evident that limited work had been done on this problem, much of it recently. Only one such solution seemed to exist for a turbulent shear layer with chemical reactions, while three solutions were found for the laminar case. It then became a matter of deciding which of these four methods appeared to have the most promise (Ref. 34 - 37). All of the methods solved the classical boundary layer equations by some numerical scheme. In addition to this search, some similar and approximate solutions were examined. By understanding the approximations, and assumptions needed for similar solutions (Ref. 38 - 42), it became clear why a nonsimilar solution was needed.

Returning to the original question after this review, it was necessary to critically compare the different approaches. In two of these methods (Ref. 34 and 36) the authors applied the straightforward technique of approximating the partial differential equations by finite difference equations and solving these algebraic equations numerically on a large computer. The main difference between these two approaches was that Zeiberg and Bleich³⁴ performed the numerical integration with an explicit scheme, whereas Blottner's work³⁶ utilized an implicit scheme.

Any explicit numerical scheme has the inherent problem of stability. In order to meet this stability criterion, the size of the step-size must be greatly reduced. This resulting reduction in the step-size greatly increases the program time on a computer to the point where it can become economically unfeasible. Blottner's method, on the other hand, is inherently stable. To achieve this stability, however, he had to solve the equations simultaneously across the entire boundary layer at station n_1 before he could proceed to station $n_1 + 1$ in the streamwise direction. To avoid the difficulty usually encountered at the stagnation point or beginning of the boundary layer, Blottner used similar profiles for the first few inches. He then was able to successfully program the solution to be accomplished in about 20 minutes.

The method in Reference 35 by Pallone et al. was quite different. They extended Dorodnitsyn's "Method of Integral Relations" to a reacting gas. This method is very similar to the Kármán-Pohlhausen concept except that the boundary layer is divided into N strips. Then the equations are integrated with respect to the normal coordinate from the wall to the edge of each strip. Polynomials with unknown coefficients were assumed for the enthalpy, concentration, and velocity profiles. Once these polynomials were integrated, ordinary differential equations in the streamwise direction remained. The values of the undetermined coefficients could then be found by integrating the set of ordinary differential equations from given initial conditions. These initial conditions were obtained from a similar solution. Pallone used a predictor-corrector technique to find the coefficients. The accuracy of

this method is greatly increased over that of the Karman-Pohlhausen method, because the equations are satisfied in the average over N subintervals of the boundary layer. Possible serious errors can occur between these intervals, however, since the concentrations change by orders of magnitude at certain times.

The final method, conceived by a group at Douglas (Ref. 37) uses a relaxation method to solve the equations. This is a double-iterative procedure which reduces the error to a minimum. Using the fluid properties at station $(n - 1)$, the momentum equation is solved at station n across the boundary layer. These properties and the solution of the momentum equation are used to solve the energy and specie equations. The enthalpy and concentration profiles are then used to calculate new fluid properties. These new properties and the solution to the original momentum equation are used to find new enthalpy and concentration profiles at station n . This iteration process is repeated until the fluid properties converge. The final fluid properties are then inserted into the momentum equation and the whole iteration process begins again. This double iteration is continued until convergence of the solution of the momentum equation is obtained. Then one can proceed to the next station and begin all over again.

After study of these methods, it was concluded that the basic scheme of Blottner's, i.e., implicit integration of a finite difference formulation would be the best choice for development of a new program. The major problems in the formulation would be expected to be the rather arbitrary description of the turbulent eddy viscosity and the treatment of more complicated chemistry, especially in the case where some

reactions are in equilibrium while others are out of equilibrium. The question of the description of eddy viscosity can be circumvented by using the ideas of Coles⁴⁵ and Crocco⁴⁶, i.e., transforming the flow to an incompressible one wherein the velocity profile is well known (at least for a boundary layer).

Shortly after reaching this point, the work done at GASL^{47, 48} was received. Rosenbaum⁴⁷ had applied an implicit integration scheme to the equations governing a turbulent boundary layer transformed in the fashion of Coles. The major problem he encountered was that certain chemical species behaved in an oscillatory fashion for reasonable step-sizes if finite reaction rates were used. This problem was resolved by Moretti⁴⁴ who linearized the chemical source terms for inviscid one-dimensional flow and examined the numerical methods of solution. Moretti was able to achieve stable solutions for greatly increased step-sizes. His solutions were then incorporated into the boundary layer problem⁴⁸ by splitting up the equation for each species into a diffusion-controlled part and a reaction-controlled part. This program thus seems to represent the best calculation scheme now available.

However, it is not without shortcomings. Specifically, Rosenbaum followed Coles in transforming only the momentum equation. The energy and specie equations were then placed in the same coordinates, Crocco⁴⁶ showed that the energy equation could itself be transformed properly and found a condition relating the Prandtl numbers of the original and transformed flows. Presumably, the specie equations could be transformed themselves giving a condition relating Schmidt numbers. These

conditions are quite complicated; however, they are satisfied identically only for $Pr = 1$ and (presumably) for $Sc = 1$. The error involved by ignoring these conditions is not obvious.

Further, Rosenbaum assumed that the turbulent Lewis number was unity. While this gives an enormous simplification, available experimental data seem consistently to give a turbulent Lewis number above unity. Whether it is practical to incorporate improvements of this nature in the GASL programs is another question, however.

Analyses of the turbulent mixing layer between two compressible gas streams have not progressed as satisfactorily as have analyses of the boundary layer on a wall. For an incompressible jet, exhausting into a quiescent medium, Prandtl's assumption of an eddy viscosity constant at each axial location and proportional to the jet centerline velocity and width correlates the experimental data quite well. However, if the jet and the receiving medium are of different density, it has been found to be necessary¹ to include the density in with the eddy viscosity. Further, if the external stream is moving, it appears that the eddy viscosity must also be a function of the axial coordinate if the form of Prandtl's assumption is to be retained⁵⁰.

Use of Prandtl's formulation (eddy viscosity proportional to velocity difference) for two-stream mixing would result in no mixing if streams of equal velocity (but unequal density) were flowing parallel. Bringing in the density as a product doesn't necessarily resolve this paradox, because then one can imagine the situation of two streams of equal ρu which would be required to remain unmixed

by this assumption. Use of ρu^2 rather than ρu as the correlation quantity suffers from a similar failing. Alpinieri⁵⁰ has carried this line of reasoning one step further by proposing a density-eddy viscosity product proportional to the sum of the ρu ratio and the ρu^2 ratio of the two streams. This procedure can only be regarded as a rather artificial and empirical one, although at this point Alpinieri's assumption may be the best one available. Incidentally, as pointed out by Mellor⁵¹, none of these mixing laws behave properly far downstream since they give an eddy viscosity increasing with downstream distance. The extension of these difficulties to reacting gases is evident.

A somewhat different approach to the turbulent mixing of two compressible streams is to try to avoid specification of the compressible eddy viscosity and instead to attempt to transform mathematically the compressible problem to an equivalent incompressible one, and then to use the relatively well established velocity profiles of the incompressible flow. Since the Coles - Crocco transformation scheme has been applied to boundary layers with considerable success, we have tried to see what results from a straight forward application of this transformation scheme to parallel mixing of two streams.

Instead of working with the differential equations as Coles did, it was decided to use the integrated conservation equations of Crocco. It became convenient to place the normal axis along the dividing streamline between the two flows. The problem then could be approached in several ways. One way was to transform the upper region separately from the

lower region, requiring that the flows in the transformed plane match at the dividing streamline. The momentum and energy equations were integrated from the dividing streamline to each outer boundary, resulting in two sets of two equations. However, it soon became evident that quantities evaluated at the dividing streamline needed to be eliminated in order to obtain a reasonable result. By integrating the conservation equations across the entire shear layer, the above problem was solved. Although, due to the nature of the integrated equations, one still had to divide the mixing layer into the same two regions, it was shown that the transformation variables had to be the same in both regions. The derivation and interpretation of the appropriate equations are given in Appendix E.

As shown in Appendix E, if we require that a constant pressure flow transform to a constant pressure flow, when $\sigma = \text{constant}$ and $\eta = \text{constant}$, and we lose the essential new feature introduced by Coles, namely, the transformation of the stream function. On the other hand, Crocco shows that for a turbulent Prandtl number of unity, a constant pressure flow must transform to a constant pressure flow (and this requirement is very nearly imposed for Prandtl numbers other than unity).

Further, application of the transformation locally tells us that⁴

$$\rho^2 \epsilon / \bar{\rho}^2 \bar{\epsilon} = \xi / \sigma \eta \quad (\text{in the nomenclature of Appendix E})$$

which says that, at any axial location $\rho^2 \epsilon = \text{constant}$, in direct contradiction with Alpinier's result, which says, at a given x ,

$$\rho \epsilon = \text{constant}.$$

Thus, from this preliminary look, we conclude that a straight-forward application of the Coles - Grosse transformation to mixing layer is not the answer and considerable further work will be required to treat mixing layers in a satisfactory fashion.

4. Possible Effects of Reactions on Turbulent Mixing Processes

As demonstrated in Section 2 of this report, the reactions which occur in the combustion product - air mixing layer release a significant amount of energy and cause sudden changes in the molecular weight of the fluid. The question then arises whether the reactions affect the turbulent transport processes themselves. Eschenroeder⁵² considered the question of the intensification of turbulence by energy releasing chemical reactions. He showed, for a system undergoing chemical reactions only, that nonequilibrium energy release contributes nothing to the vortical component of the turbulence - the effect is combined to the dilational component.

Since in our problem of turbulent mixing we are interested in the transport of vorticity, we have re-examined Eschenroeder's work to investigate its generality.

Eschenroeder considers the interaction of chemical reactions with an isolated element of the vortical component of the fluctuating flow. The circulation theorem and vorticity conservation law are obtained in a general manner as:

$$\frac{D}{Dt} \oint_{\tau} \vec{q} = \oint_{\tau} \frac{D \vec{q}}{Dt} d\vec{\ell} + \oint_{\tau} \vec{q} \frac{D}{Dt} (d\vec{\ell})$$

where \vec{q} = velocity, $d\vec{\ell}$ = element of length along contour τ enclosing a simply connected region (S) , and

$$\frac{D}{Dt} = \frac{\partial}{\partial t} + \vec{v} \cdot \nabla$$

is the particular derivative. If the Reynolds number is large, the momentum equation is

$$\frac{D}{Dt} \vec{g} = - \frac{1}{\rho} \nabla p$$

so

$$\frac{D}{Dt} \vec{g} = - \oint_{(S)} (\nabla \times \frac{\vec{v} p}{\rho}) d\vec{A}$$

using the Stokes theorem.

The thermodynamic equation expresses $\frac{D}{Dt} p$ in terms of state variables. Following Clarke and Mc Chesney's⁵⁴ general form, the thermodynamic equation reads as

$$de = T_1 dS + \sum_{\nu=2}^M \sum_{\alpha=1}^N (T_{\alpha\nu} - T_1) d(e_{\alpha\nu} S_{\alpha\nu}) - p d(\frac{1}{\rho}) + \sum_{\alpha=1}^N \mu_{\alpha} d\alpha$$

where the influence of the internal modes is summarized in the $(\sum \sum)$ term, and in the chemical potentials:

$$\mu_{\alpha} = \mu_{\alpha 1} + \sum_{\nu=2}^M \mu_{\alpha \nu}$$

$$\mu_{\alpha \nu} = e_{\alpha \nu} - T_{\alpha \nu} S_{\alpha \nu}$$

where subscripts

1 corresponds to the translational mode

ν to other modes, $2 \dots m = \nu$

α refers to the chemical species, $1 \dots n$

and where c denotes the mass concentration.

Thus

$$-\frac{\nabla p}{\rho} = T_1 \nabla S - \nabla h + \sum_{\nu=2}^m \sum_{\alpha=1}^n (T_{\alpha\nu} - T_1) \nabla (c_{\alpha} S_{\alpha\nu}) + \sum_{\alpha=1}^n \mu_{\alpha} \nabla c_{\alpha}$$

$$\text{and } \frac{D\vec{r}}{Dt} = \oint_{(S)} \left[\nabla \times (T_1 \nabla S - \nabla h + \dots + \sum_{\alpha=1}^n \mu_{\alpha} \nabla c_{\alpha}) \right] d\vec{A}$$

in the most general form.

Now for each species, we have

$$\frac{\partial \mu_{\alpha}}{\partial T}_{p, c_p} = \frac{\mu_{\alpha} - h_{\alpha}}{T} = -S_{\alpha}$$

or

$$\mu_{\alpha} = h_{\alpha} - T S_{\alpha}$$

more exactly,

$$\mu_{\alpha} = h_{\alpha} - \sum_{\nu=1}^m T_{\alpha\nu} S_{\alpha\nu}$$

$$h_{\alpha} = e_{\alpha 1} + \frac{p_{\alpha}}{\rho_{\alpha}} + \sum_{\nu=2}^m e_{\alpha\nu}$$

since $T_{\alpha 1} = T_1$, the translational-mode temperature.

Also,

$$\begin{aligned} \sum_{\alpha=1}^n \mu_{\alpha} \nabla c_{\alpha} &= \sum_{\alpha=1}^n (h_{\alpha} - \sum_{\beta=2}^m T_{\alpha\beta} S_{\alpha\beta}) \nabla c_{\alpha} \\ &= \sum_{\alpha=1}^n h_{\alpha} \nabla c_{\alpha} - \sum_{\alpha=1}^n \sum_{\beta=2}^m (T_{\alpha\beta} S_{\alpha\beta}) \nabla c_{\alpha} \end{aligned}$$

Thus the bracketed term of the integral becomes

$$\begin{aligned} (A) \quad & \left[\nabla \times \left\{ T_1 \nabla S - \nabla h + \sum_{\alpha=1}^n \sum_{\beta=2}^m (T_{\alpha\beta} - T_1) \nabla (c_{\alpha} S_{\alpha\beta}) \right. \right. \\ & \left. \left. + \sum_{\alpha=1}^n h_{\alpha} \nabla c_{\alpha} - \sum_{\alpha=1}^n \sum_{\beta=1}^m (T_{\alpha\beta} S_{\alpha\beta}) \nabla c_{\alpha} \right\} \right] \end{aligned}$$

So it seems that, to reach the conclusions attained by Eschenroeder, namely that "the irreversible contribution of composition changes is explicitly excluded, and the only sources of coupling that may occur between chemistry and vortical component of the flow are those which act through the influence of p and T ," it is necessary to assume that there is no raise of energy due to relaxation of the internal modes of the gas.

If the internal modes are neglected, we obtain Eschenroeder's expression

$$\frac{D\vec{\Gamma}}{Dt} = \oint_{(S)} \left[\nabla T \times \nabla S - \nabla T \times \sum_i S_i \nabla c_i \right] d\vec{A}$$

where effectively the contribution of chemical changes disappears.

But in the case of a gas with internal relaxation modes $(s_{\alpha\beta})$, $T_{\alpha\beta}$ are not constant, and we cannot reach the same conclusion. Going back to expression (A), decompose $\{\dots\}$ into

Enthalpy terms

$$\left[\nabla h = \sum_{\alpha=1}^n h_{\alpha} \nabla c_{\alpha} \right] \quad \text{and}$$

Entropy terms

$$T_1 \nabla s + \sum_{\alpha=1}^n \sum_{\beta=2}^m T_{\alpha\beta} \nabla (c_{\alpha} s_{\alpha\beta}) = \sum_{\alpha=1}^n \sum_{\beta=2}^m c_{\alpha} \nabla (c_{\beta} s_{\alpha\beta})$$

1

2

3

$$= \sum_{\alpha=1}^n T_1 s_{\alpha 1} \nabla c_{\alpha} + \sum_{\alpha=1}^n \sum_{\beta=2}^m (T_{\alpha\beta} s_{\alpha\beta}) \nabla c_{\alpha}$$

4

5

Use

$$T_{\alpha\beta} \nabla (c_{\alpha} s_{\alpha\beta}) = T_{\alpha\beta} c_{\alpha} \nabla s_{\alpha\beta} + T_{\alpha\beta} s_{\alpha\beta} \nabla c_{\alpha}$$

to combine terms 2 and 5, which gives

$$\sum_{\alpha=1}^n \sum_{\beta=2}^m (T_{\alpha\beta} c_{\alpha} \nabla s_{\alpha\beta})$$

while the third and fourth terms give

$$= T_1 \nabla s + \sum_{\alpha=1}^n T_1 c_{\alpha} (\nabla s_{\alpha 1})$$

and, finally,

$$\frac{D\vec{\Gamma}}{Dt} = \oint_{(S)} \nabla \times \left\{ \sum_{i=1}^N \sum_{j=1}^M T_{ij} c_{ij} \nabla (\phi_{ij}) \right\} d\vec{A}$$

This result demonstrates that in fact chemical reactions, when associated with internal state transitions, will give rise to the production of vorticity.

Obviously, in the equilibrium case, the entropy is constant for any element of gas in these circumstances, all $T_{ij} = T_1$, and the induced vorticity will be zero. The vorticity will be zero also if the flow is all frozen, or if the chemical reactions are frozen and the internal states are in equilibrium, or vice versa.

Now let us look at the possible effect of reaction-associated molecular weight changes on turbulent transport. To get an idea of how such an effect might arise, we go back to the simple physical description afforded by Prandtl's mixing length theory. For reference, we first review the results of mixing length theory which we will use.

Consider parallel flow in which the velocity varies only from streamline to streamline.

$$\begin{aligned} \text{Let } \quad \bar{u} &= \bar{u}(y) & \text{along } \vec{x} - \text{axis} \\ \bar{v} &= \bar{w} = 0 \end{aligned}$$

As the fluid passes along streamlines in turbulent motion, fluid particles coalesce into lumps which move bodily, and cling together for a given traversed length, in longitudinal and transverse directions, while retaining momentum parallel to the \vec{x} -axis.

Prandtl assumes that such a lump of fluid which comes from the layer $(y_0 - \ell)$, with velocity $\bar{u}(y_0 - \ell)$ is displaced over a length ℓ

in the transverse direction. The distance ℓ is known as Prandtl's mixing length.

The difference of velocity will be

$$\Delta \bar{u}_1 = \bar{u}(y_0) - \bar{u}(y_0 - \ell)$$

which reads, if a Taylor expansion around y_0 is used (first order)

$$\Delta \bar{u}_1 = \ell \left(\frac{d\bar{u}}{dy} \right)_{y_0}$$

Similarly, for a lump of fluid coming from $y_0 + \ell$ to y_0 :

$$\Delta \bar{u}_2 = \ell \left(\frac{d\bar{u}}{dy} \right)_{y_0}$$

In the first case we had $v^x > 0$, in the second $v^x < 0$ for the transverse motion.

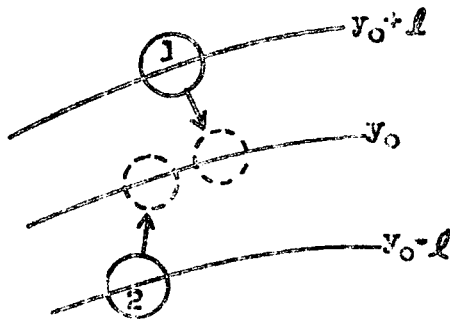
The time average of the absolute value of the fluctuation will be

$$|\bar{u}^x| = \frac{1}{2} (|\Delta \bar{u}_1| + |\Delta \bar{u}_2|) = \ell \left| \frac{d\bar{u}}{dy} \right|_{y_0}$$

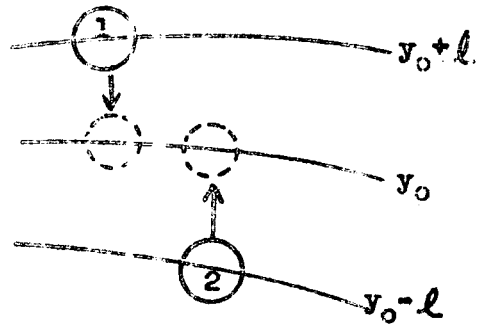
So the mixing length ℓ is the distance (transverse) which must be covered by a lump of fluid traveling with its original mean velocity, in order to make the difference between its velocity and the new velocity of the new position equal to the mean transverse fluctuation in turbulent flow.

If we consider two lumps meeting at the lamina y_0 , the first one comes from $y_0 + \ell$, the other one from $y_0 - \ell$. Two cases may take place:

(A)



(B)



In both cases fluid 1 is assumed to be moving faster than fluid 2. In case A, the two lumps will go diverging with a velocity $(2 \bar{u}')$; the empty space between them has to be filled by surrounding fluid. In case B, the lumps will collide (with velocity $2 u'$) and then recoil sideways.

In both cases, this gives rise to a transverse velocity component, and this transverse component v' has to be of the same order of magnitude as u' , and

$$|\bar{v}'| = c \times l \left(\frac{d\bar{u}}{dy} \right)_{y_0}$$

Considering that in any case the product $u' v'$ is negative a $(> 0) u'$ comes from a $(< 0) v'$ and vice versa and we have

$$\overline{u' v'} = -c |\bar{u}'| \cdot |\bar{v}'| = -l^2 \left(\frac{d\bar{u}}{dy} \right)^2$$

the constant being included in the mixing length.

The shearing-stress is then

$$\tau_{xy} = \tau = -\rho \overline{u' v'} = \rho l^2 \left(\frac{d\bar{u}}{dy} \right)^2$$

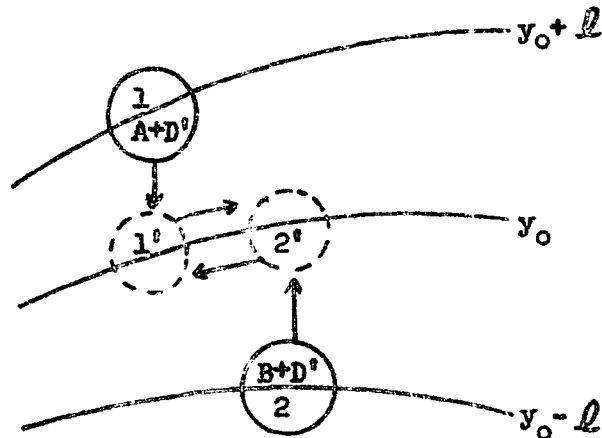
which will have to be added in the general stress tensor to get the Navier-Stokes equation in this case.

A generalization of this concept consists of including the existence of chemical reaction, and therefore changes of molecular weight.

We consider each lump of fluid submitted to transverse motion as consisting of a mixture of different chemical species. When two lumps arrive at contact, these species can react with each other, thus causing a change in density, and affecting the balance of momentum across the layer y_0 .

In a general case, we can take two lumps of fluid, the first one at the layer $(y_0 + \ell)$, is made of a mixture $A + D^0$, the second at the layer $(y_0 - \ell)$, is made of $B + D^0$.

The reaction $A + B \rightarrow C$ can occur, and we suppose that D^0 is inert with respect to this reaction.



The masses of the respective lumps are:

$$m_1 = \rho_1 V_1 = N_{x1} M_A + N_{z1} M_{D^0}$$

$$m_2 = \rho_2 V_2 = N_{y2} M_B + N_{z2} M_{D^0}$$

$$m_1' = \rho_1' V_1' = N_{x1}' M_A + N_{z1}' M_{D^0} + k_1 M_C$$

$$m_2' = \rho_2' V_2' = N_{y2}' M_B + N_{z2}' M_{D^0} + k_2 M_C$$

Where it is assumed that the product of reaction, C, obeys ideal gas law, on k_1 to k_2 and is proportional n_1 to n_2 , and the symbols are:

$$\begin{aligned} n &= \text{volume} & N &= \text{number of molecules} \\ \rho &= \text{density} & M &= \text{molecular weight} \end{aligned}$$

By applying conservation of the atoms, we get

$$N_{x1} - N_{x1} = N_{y2} - N_{y2} = -n$$

$$n = k_1 + k_2$$

$$N_{x1} + N_{x2} = N_{y1} + N_{y2}$$

Now, the exchange of momentum occurring during the transformation of the liquid, respectively from $(y_0 + l)$ to y_0 and $(y_0 - l)$ to y_0 will be

$$\begin{aligned} \Delta p &= n_1 u (y_0 + l) + n_2 u (y_0 - l) + u (y_0) [n_1^0 - n_2^0] \\ &= u_0 \left[n_1 - n_1^0 + n_2 - n_2^0 \right] + l \frac{\rho u}{2} (n_1 - n_2) \end{aligned}$$

or

$$\begin{aligned} \Delta p &= \left[\rho (M_A - M_B) + \rho M_0 (N_{x1} - N_{y2}) + M_0 (N_{x2} - N_{y1}) \right] u_0 \\ &+ \left[N_{x1} M_A + N_{y2} M_B + (N_{x2} + N_{y1}) M_0 \right] l \frac{\rho u}{2} u_0 \end{aligned}$$

in terms of molecular weights.

It can be seen that the second bracketed terms correspond to the terms that in the first term correspond to $\Delta \rho$ by a volume ΔV and density ρ of the mixture. However, we do get an additional term $u(y_0)$ in the change of momentum Δp .

Still, we can say that u^2 varies as $\Delta \rho$ and the magnitude of magnitude. The shearing stress τ will now be

$$\tau = \frac{M_{z1} + I_{z2} M_{z2} + (M_{z1} + I_{z2} M_{z2})}{2 (I_{z1} + I_{z2})} \left(\frac{\partial u}{\partial y} \right)^2$$

$$= \left[\frac{k (M_{z1} + M_{z2}) + 2 M_{z2} (M_{z1} + M_{z2}) + I_{z2} (M_{z1} + M_{z2})}{2 (I_{z1} + I_{z2})} \right] \left(\frac{\partial u}{\partial y} \right)^2$$

or

$$\tau = A \left(\frac{\partial u}{\partial y} \right)^2 + B \left(\frac{\partial u}{\partial y} \right)^2$$

A and B can be expressed in terms of the shear modulus G and ρ , $\Delta \rho$, ΔV of each lump and each species. But then we have to make some assumptions in order to simplify the equations.

We can assume that the reaction does not affect the composition of the fluid (dilute reactants). We could assume that each lump just reacts with the other, but that there is no exchange of $\Delta \rho$ between in the collision. Then we drop out the term

$$2 M_{z2} (I_{z1} + I_{z2})$$

in the second bracketed term.

Also, we have to find a distribution law for the product $\bar{u} \bar{v}$ in order to derive k_1 and k_2 .

In any event, it seems that reactions are likely to affect the momentum transport, since the momentum equation now is:

$$\bar{\rho} \bar{u} \frac{\partial \bar{u}}{\partial x} + \bar{\rho} \bar{v} \frac{\partial \bar{u}}{\partial y} = \frac{\partial}{\partial y} \left[\mu \frac{\partial \bar{u}}{\partial y} + A L^2 \left(\frac{\partial \bar{u}}{\partial y} \right)^2 + \tau \bar{u} \right]$$

In order to get an idea on the probability for such two lumps to encounter each other, and for the reaction to take place, some characteristic times of the turbulent motion and chemical reaction can be compared.

Taking the spectral representation of the turbulent flow, in which the motion consists of eddies of different size and frequencies, each characterized by its wave-number, we can define a characteristic time of the eddy by dimensional analysis. This time has to be constructed of the wave number characterizing the eddy and the spectral energy associated with it.

The dimensions are:

for the three-dimensional energy spectrum $[E] = L^3 U^{-2}$

for the wave-number $[k] = L^{-1}$

So we can let

$$\tau_T = [k^3 E(k)]^{-\frac{1}{2}}$$

be the characteristic time of the turbulence, as suggested by Corrsin and Taylor.

Now the energy spectrum has been expressed in terms of the wave number by Kolmogorov and Heisenberg as

$$E(k) = \epsilon^{2/3} k^{-5/3}$$

for the "middle range of k " where the similarity hypothesis of Kolmogorov is valid, i.e., large eddies, almost in statistical equilibrium, with negligible viscous effects.

ϵ is the rate of dissipation of turbulent energy.

In the larger range of k , we have $E(k) \sim k^{-7}$. Now to define a chemical relaxation time, in the same way, we follow Corrsin⁵⁸ who studied the turbulent mixing with isothermal first and second order reactions.

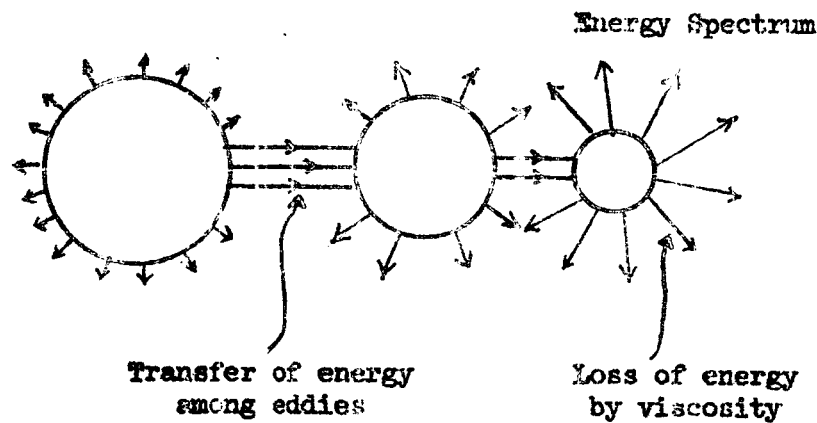
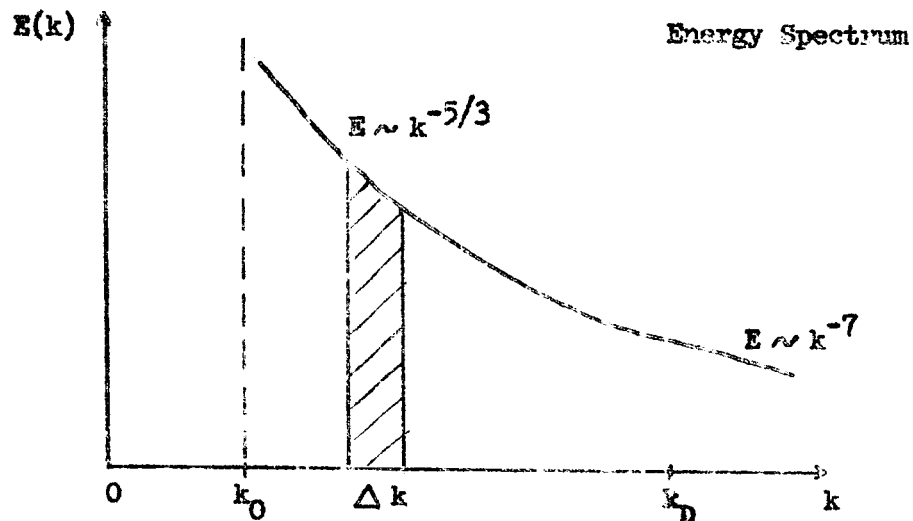
Corrsin defines dimensionally a characteristic time corresponding to the reactive transfer rate. This time must depend on the local concentration spectrum, on the reaction rate constant, and on the wave number k .

$$\tau_R = [k C^2 G]^{-1/2}$$

Where G is the Fourier spectrum of the concentration field and C is the reaction rate constant. Using the Osage's cascade model, Corrsin derives the form of G in terms of k .

The redistribution of the turbulent energy among more and more Fourier components of the velocity field, related to ever increasing wave-numbers, can be schematized in a "cascade process," where the

energy of the turbulence passes from larger to smaller eddies (i.e. increase of each eddy losing an amount of energy (due to viscosity) which is increasing with k).



in this direction ...

- k increases
- size of eddy decreases
- energy dissipated increases
- Re decreases (viscosity increases)

The spectral energy transported in a step will be

$$[E(k) \cdot \Delta k] \quad \text{Onsager takes a step length } \Delta k = k$$

(the sequence of wave numbers will
be a geometric progression)

So the flux $F(k)$ past any wave-number is of the order

$$F(k) \sim \frac{E(k) \cdot k}{\tau(k)} \quad \tau \text{ being characteristic time of the turbulent motion.}$$

If we neglect viscous dissipation, our cascade is conservative and $F(k)$ must be constant

$$\frac{dF}{dk} = 0$$

This actually will give $F = \epsilon$ and then

$$E(k) = \epsilon^{2/3} k^{-5/3}$$

which is the Kolmogorov's result for the inertial range of the energy spectrum.

Corrsin has extended this model to a non-conservative system:

$$\frac{dF}{dk} = \left\{ \text{rate of gain of spectral content per unit } k \right\}$$

and applying this to the concentration spectrum G , Corrsin gets

$$G(k) \sim B k^{-5/3} \exp \left\{ 3 C \epsilon^{-1/3} k^{-2/3} \right\}$$

for the inertial convective range (middle range of k , where diffusion is neglected).

The same derivation has been made for the inertial diffusive range, but there the results of Corrsin, namely

$$G(k) \sim k^{-5/3} \exp \left[3 C \epsilon^{-1/3} k^{2/3} - \frac{3}{2} D \epsilon^{1/3} k^{4/3} \right]$$

does not agree with the previously attained result of Taylor,

$$G \sim k^{-17/3}$$

We can therefore sensibly compare the characteristic times of chemical and turbulence spectra only for the inertial convective range, or middle range of k , again neglecting diffusion effects.

$$\tau_T = (\epsilon^{1/2} k)^{-2/3}$$

and

$$\tau_R = k^{-1/2} \epsilon^{-1} G^{-1/2}$$

Applying the Onsager cascade model method to the three dimensional spectrum of the field of containment (supposed stationary, locally isotropic), we have the flux past any wave-number k

$$F \sim \frac{k G(k)}{\tau(k)}$$

then the equation

$$\frac{dF}{dk} = \left\{ \text{rate of gain of spectral content per unit } k \right\}$$

gives

$$\frac{d}{dk} \left\{ \epsilon^{1/3} k^{5/3} G \right\} = -2 C_1 G$$

which yields the solution

$$G = \epsilon_0 C^{3/2} (k \epsilon^{1/2})^{-5/3} \exp \left\{ 3 C (k \epsilon^{1/2})^{-2/3} \right\}$$

ϵ_0 being the small k "initial" flux of $\bar{\phi}^2$ contained into the spectrum.

Thus τ_R can be expressed as

$$\tau_R = k^{-1/2} C^{-1} \epsilon_0^{-1/2} C^{-3/4} (k \epsilon^{1/2})^{5/6} \exp \left\{ -\frac{3}{2} C (k \epsilon^{1/2})^{-2/3} \right\}$$

$$\tau_R = \epsilon_0^{-1/2} k^{-1/2} C^{-7/4} (k \epsilon^{1/2})^{5/6} \exp \left\{ -\frac{3}{2} C (k \epsilon^{1/2})^{-2/3} \right\}$$

we can substitute $\tau_T \approx (k \epsilon^{1/2})^{-2/3}$ in this expression, then

$$\tau_R \approx \epsilon_0^{-1/2} k^{-1/2} C^{-7/4} \tau_T^{-5/4} \exp \left\{ -\frac{3}{2} C \tau_T \right\}$$

There, assuming that $C \tau_T$ is small, we can take the exponential as nearly unity, or take the expansion

$$e^{-\frac{3}{2} C \tau_T} \approx 1 - \frac{3}{2} C \tau_T + \left(\frac{9}{8} C^2 \tau_T^2 - \frac{27}{16} C^3 \tau_T^3 + \dots \right)$$

then

$$\tau_R \approx \epsilon_0^{-1/2} k^{-1/2} C^{-7/4} \left[\tau_T^{-5/4} - \frac{3}{2} C \tau_T^{-1/4} + \frac{9}{8} C^2 \tau_T^{3/4} - \dots \right]$$

or

$$\frac{\tau_H}{\tau_T} \approx \epsilon^{-1/2} k^{-1/2} C^{-7/4} \tau_T^{-9/4}$$

the ratio $\frac{\tau_H}{\tau_T}$ goes to zero as k goes to ∞ and decreases as k increases, and goes to infinity as C goes to zero, and decreases as C increases. Note that this expression is valid only for the middle range of k , corresponding to the inertial convective region of the spectrum.

The ratio will be small only if C is quite large, since τ_T is small and k is small.

Another approach is used by Corrsin to estimate the dimensional coefficient B in the expression of $G(k)$.

$$G(k) \approx B k^{-5/3} \exp \left\{ 3 C \epsilon^{-1/3} k^{-2/3} \right\} \quad (1)$$

and

$$\overline{\theta^2} = \int_0^\infty G dk \approx \int_{\epsilon^{k_L}}^{\epsilon^{k^*} \text{ or } \infty} G dk \quad (2)$$

where ϵ^{k_L} is the "energy bearing" wave-number and ϵ^{k^*} represents the end of the inertial convective range.

The limitation of this process is that the main contribution to the integral comes from the region near ϵ^{k_L} , where G is not well approximated by the expression (1).

By integration, (2) becomes

$$\overline{\theta^2} \approx - \frac{B \epsilon^{1/3}}{2 C} \left[- \exp \left\{ 3 C \epsilon^{-1/3} \epsilon^{k_L - 2/3} \right\} \right]$$

or

$$B \approx 2 C \bar{\theta}^2 \epsilon^{-1/3} \exp \left\{ - 3 C \epsilon^{-1/3} \bar{\theta}_L^{k-2/3} \right\}$$

For $C \rightarrow 0$, Corrsin obtains by expanding this as a series

$$B \rightarrow \frac{2}{3} \bar{\theta}^2 \bar{\theta}_L^{k-2/3}$$

This gives only the dimension of B and not a way of evaluating its value.

5. Future Work

During the next reporting period, we plan to investigate further the transformation of the high speed reacting mixing layer into a simpler low speed analogue. The effects of non-equilibrium reactions on the viscous-inviscid interaction which occurs in base flows will be considered. The fluid mechanic structure of the recirculating flow region will be investigated along with analytical techniques to describe this region. The effects of chemical reactions on turbulent transport processes will be examined further.

6. Personnel

Mr. E. Palmreuter has been awarded a National Science Foundation Traineeship for the 1965-66 school year. Thus, he will be unable to continue on this project during this school year. Mr. F. F. Luo has been added to the project staff. He is working towards a Ph. D. degree in Aeronautical Engineering; he was awarded the M. S. degree by the University of Detroit in January, 1965.

References

1. Ferri, A., Libby, P. A. and Zakkay, V. "Theoretical and Experimental Investigation of Supersonic Combustion" Aeronautical Research Laboratories No. 62-467, Sept. 1962.
2. Ferri, A., Libby, P. A. and Zakkay, V. "Theoretical and Experimental Investigation of Supersonic Combustion" Aeronautical Research Laboratories No. 62-467, pp. 82-83, Sept. 1962.
3. Westenberg, A. A. and Favin, S. "Complex Chemical Kinetics in Supersonic Nozzle Flow" Ninth Symposium on Combustion, 1962 pp. 785-789, Academic Press.
4. Rozsa, R. B. "Preliminary Review of Turbulent Jet-Mixing and Afterburning in Rocket Exhaust Plumes" Chrysler Corp. Technical Bulletin TB-AE-64-79, Nov. 1964.
5. Feigenbutz, L. V. "Turbulent Mixing and Combustion of a Rocket Exhaust Jet with Surrounding Atmosphere, Part I The Balanced Jet" General Dynamics/Astronautics AE 63-0024, Dec. 1962.
6. Vasiliu, J. "Turbulent Mixing of a Rocket Exhaust Jet With a Supersonic Stream Including Chemical Reactions" Jour. Aerospace Sci. Vol. 29, No. 1, pp. 19-23, Jan. 1962.
7. Feigenbutz, L. V. "Turbulent Mixing and Combustion of a Rocket Exhaust Jet With the Surrounding Atmosphere, Part II A The Near Field of an Initially Unbalanced Jet" General Dynamics/Astronautics GDA 63-0030, April 1963.
8. Lin, S. C. and Hayes, J. E. "A Quasi-One-Dimensional Treatment of Chemical Reactions in Turbulent Wakes of Hypersonic Objects" AIAA Jour. Vol. 2, No. 7, pp. 1215-1222, July 1964.
9. Kaskan, W. E. "Hydroxyl Concentrations in Rich Hydrogen-Air Flames Held on Porous Burners" Combustion and Flame, Vol. 2, No. 3, pp. 229-243, Sept. 1958.
10. Kaskan, W. E. "The Concentration of Hydroxyl and of Oxygen Atoms in Gases From Lean Hydrogen-Air Flames" Combustion and Flame, Vol. 2, No. 3, Sept. 1958.
11. Rozsa, R. B. Extension of Ref. 4, To Be Published.

12. Kaskan, W. E. and Browne, W. G. "Kinetics of the $H_2/CO/O_2$ System" General Electric Missile and Space Division Report, RG4SD37, July 1964.
13. Gaydon, A. G. "The Spectroscopy of Flames" Chapman and Hall, London, Chapter 6, 1957.
14. Leah, A. S. and Watson, H. "Radiation from Explosion Flames of Carbon Monoxide" Combustion and Flame, Vol. 3, No. 2, pp. 169-186, 1958.
15. Westenberg, A. A. and Fristrom, R. M. "Methane-Oxygen Flame Structure, Part IV, Chemical Kinetic Considerations" J. Phys. Chem., Vol. 65, pp. 591, 1961.
16. Kaskan, W. E. "The Source of the Continuum in Carbon Monoxide-Hydrogen-Air Flames" Combustion and Flame, Vol. 3, No. 1, pp. 39-48, 1959.
17. Clyne, M. A. A. and Thrush, B. A. "Mechanism of Chemiluminescent Combination Reactions Involving Oxygen Atoms" Proceedings of the Royal Society of London, Series A, Vol. 264, pp. 404-418, 1962.
18. Kaskan, W. E. "Excess Radical Concentrations and the Disappearance of Carbon Monoxide in Flame Gases From Some Lean Flames" Combustion and Flame, Vol. 3, No. 2, pp. 49-59, 1959.
19. Gibson, W. "The Effect of Ambient Dissociation and Species Diffusion of Non-Equilibrium Shock Layers" Presented at I.A.S. 31th Annual Meeting, New York, Jan. 21-23, 1963, I.A.S. Paper No. 63-70.
20. Westenberg, A. A. Private Communication.
21. Reference 13, pp. 189.
22. Høglund, R. F., Carlson, D. and Byron, S. "Experiments on Recombination Effects in Nozzles" AIAA Jour., Vol. 1, No. 2, pp. 324-328, Feb. 1963.
23. Fenimore, C. P. and Jones G. W. "The Decomposition of Ethylene and Ethane in Premixed Hydrocarbon-Oxygen-Hydrogen Flames" Proceedings Ninth (International) Symposium on Combustion, Academic Press, pp. 597-603, 1962.
24. Kaufman, F. and Delgreco, F. P. "Fast Reactions of OH Radicals" Proceedings Ninth (International) Symposium on Combustion, Academic Press, pp. 659-665, 1962.

25. Wise, H. and Rosser, W. A. "Homogeneous and Heterogeneous Reactions of Flame Intermediates" Proceedings Ninth (International) Symposium on Combustion, Academic Press, pp. 733-742, 1962.
26. Fenimore, C. P. and Jones, G. W. "Acetylene in Flames With Oxygen" J. Chem. Phys., Vol. 39, No. 6, pp. 785-798, 15 Sept. 1963.
27. Monteiloff, I. N., Taback, E. D. and Buswell, R. F. "Kinetics of Hydrogen-Air Flow Systems, I, Calculation of Ignition Delay for Hypersonic Ramjets" Proceedings Ninth (International) Symposium on Combustion, Academic Press, pp. 220-230, 1962.
28. Brabbs, T. A., Belles, F. E. and Zlatarich, S. A. "Shock Tube Study of Carbon Dioxide Dissociation Rate" J. Chem. Phys., Vol. 38, No. 8, pp. 1939-1944, April 1963.
29. Mahan, B. H. and Solo, R. B. "Carbon Monoxide-Oxygen Atom Reaction" J. Chem. Phys., Vol. 37, No. 11, pp. 2669-2677, Dec. 1962.
30. Boynton, F. P. "Chemical Kinetic Analysis of Rocket Exhaust Temperature Measurements" AIAA Jour., Vol. 2, No. 3, pp. 577-578, March 1964.
31. Kurzius, S. C. "Rocket Exhaust Neutral and Ionized Species Reaction Mechanism" Report TP-114, Aero. Chem. Research Laboratories, Inc., April 1965.
32. Fenimore, C. P. and Jones, G. W. "The Reaction of Hydrogen Atoms with Carbon Dioxide at 1200-1350 °K" J. Phys. Chem., Vol. 62, pp. 1578, Dec. 1958.
33. Clyne, M. A. A. and Thrush, B. A. "The Kinetics of the Carbon Monoxide Flame Bands" Proceedings Ninth (International) Symposium on Combustion, Academic Press, pp. 177-183, 1962.
34. Zeiberg, S. L. and Bleich, G. D. "Finite Difference Calculation of Hypersonic Wakes" AIAA Jour., Vol. 2, pp. 1396-1402 Aug. 1964.
35. Pallone, A. J., Moore, J. A. and Erdos, J. I. "Nonequilibrium, Nonsimilar Solutions of the Laminar Boundary Layer Equations" AIAA Preprint No. 64-60.
36. Blottner, F. G. "Nonequilibrium Laminar Boundary Layer Flow of a Binary Gas" G.E. Report R 63 S 017, also AIAA Jour. Vol. 2, pp. 232-240, Nov. 1964.
37. Clutter, D. A., Smith, A. M. and Jaffee, N. A. "General Method for Solving Nonequilibrium Laminar-Boundary-Layer Flow of a Binary Gas" Douglas Aircraft Division Report No. LB 31616, Oct. 1964.

38. Rae, W. F. "Approximate Solution for Nonequilibrium Boundary Layer Near the Leading Edge of a Flat Plate" *IAI Paper* 62-178, June 1962.
39. Brainerd, J. J. and Levinsky, E. S. "Viscous and Nonviscous Flows with Finite-Rate Chemical Reactions" *IAI Paper* 63-52, 1963.
40. Casaccio, A. "Similar Solutions for Laminar Mixing of Reactive Gases" *AIAA Jour.* Vol. 2, pp. 1403-1409, Aug. 1964.
41. Casaccio, A. and Cousin, S. "A Simple Approach to the Multicomponent Laminar Boundary Layer" *AIAA Jour.* Vol. 3, pp. 756-758, April 1965.
42. Bloom, M. H. and Steiger, M. H. "Further Similarity Solutions of Axisymmetric Wakes and Jets" *AIAA Jour.* Vol. 3, pp. 548-550, Mar. 1965.
43. Libby, P. A., Rosenbaum, H. and Slutsky, S. "The Laminar Boundary Layer in Hydrogen-Air Mixtures with Finite Rate Chemistry" *General Applied Science Laboratories TR 385*, Nov. 1963.
44. Moretti, G. "A New Technique for the Numerical Analysis of Nonequilibrium Flows" *AIAA Jour.* Vol. 3, pp. 223-229, Feb. 1965.
45. Coles, D. E. "The Turbulent Boundary Layer in a Compressible Fluid" *Rand Corp. Report R-403-JR*, 1962.
46. Crocco, L. "Transformations of the Compressible Turbulent Boundary Layer with Heat Exchange" *AIAA Jour.* Vol. 1, pp. 2725-2731, Dec. 1963.
47. Rosenbaum, H. "Compressible Turbulent Boundary Layer with Application to Hydrogen Dumping and Combustion" *General Applied Science Laboratories TR 514*, March 1965.
48. Slutsky, S. and Rosenbaum, H. "Laminar Boundary Layer Calculations with Finite Rate Chemistry" *General Applied Science Laboratories TR 516*, March 1965.
49. Casaccio, A. "Turbulent Mixing of Reactive Gases" *AIAA Jour.* Vol. 3, pp. 1160-1162, June 1965.
50. Alpinieri, L. J. "Turbulent Mixing of Coaxial Jets" *AIAA Jour.* Vol. 2, pp. 1560-1567, Sept. 1964.
51. Mello, G. L. "Comments on 'Turbulent Mixing of Coaxial Jets'" *AIAA Jour.* Vol. 3, p. 796, April 1965.

52. Eschenroeder, A. Q. "Intensification of Turbulence by Chemical Heat Release" GM Defense Research Laboratories TR 63-217D Aug. 1963.
53. Hinze, J. O. "Turbulence - An Introduction to its Mechanism and Theory" McGraw-Hill, New York, 1959.
54. Clarke, J. F. and McChesney, M. "The Dynamics of Real Gases" Washington, Butterworths, 1964.
55. Schlichting, H. "Boundary Layer Theory" McGraw-Hill, New York
56. Pai, S. I. "Turbulent Flow Theory " D. Van Nostrand, New York
57. Onsager, L. Nuovo Cimento Suppl. 6, No. 2, p. 279, 1949.
58. Corrsin, S. The Physics of Fluids Vol. 7, No. 8, Aug. 1964.
59. Batchelor, G. K. J. Fluid Mech. Vol. 5, No. 113, p. 134, 1959.

Appendix A Discussion of Reactions for

Kaskan and Browne¹² have accomplished a literature search for the kinetic data of the more important chemical reactions in the hydrogen-carbon monoxide-oxygen system. They arrived at a set of twenty-one reactions involving eleven different chemical species. Their chemical reactions are shown in Table A-I. Certain reactions shown in Table A-I were not considered in the present analysis.

Reaction D ($\text{OH} + \text{OH} \rightleftharpoons \text{H}_2 + \text{O}_2$) was dropped because no experimental data was found on this reaction. Also, the same net effect is produced by reactions B and C.

Reaction F ($\text{H}_2 + \text{O}_2 \rightleftharpoons \text{H}_2\text{O} + \text{O}$) was dropped, because no information on its rate was found and it is thought that reaction E will be the main producer of $\text{H}_2\text{O} + \text{O}$.

Reaction K ($\text{O} + \text{O}_2 + \text{M} \rightleftharpoons \text{O}_3 + \text{M}$) was dropped. It was assumed that the concentration of O_2 will be very low in the primary reaction zone; O_3 was neglected throughout the plume.

Reactions L - O were not considered to be important. This has been the general rule in flame studies because of the instability of the H_2O_2 and HO_2 molecules.

Kaskan and Browne¹² state that it has been shown that the recombination of OH is apparently second order in OH and independent of pressure, which implies that it does not involve a third body.

Table A-I Possible Chemical Reactions

$\text{OH} + \text{H}_2$	$\text{H}_2\text{O} + \text{H}$	A
$\text{H} + \text{O}_2$	$\text{OH} + \text{O}$	B
$\text{O} + \text{H}_2$	$\text{OH} + \text{H}$	C
$\text{OH} + \text{OH}$	$\text{H}_2 + \text{O}_2$	D
$\text{OH} + \text{CH}$	$\text{H}_2\text{O} + \text{O}$	E
$\text{H}_2 + \text{O}_2$	$\text{H}_2\text{O} + \text{O}$	F
$\text{H} + \text{H} + \text{M}$	$\text{H}_2 + \text{M}$	G
$\text{H} + \text{OH} + \text{M}$	$\text{H}_2\text{O} + \text{M}$	H
$\text{H} + \text{O} + \text{M}$	$\text{OH} + \text{M}$	I
$\text{O} + \text{O} + \text{M}$	$\text{O}_2 + \text{M}$	J
$\text{O} + \text{O}_2 + \text{M}$	$\text{O}_3 + \text{M}$	K
$\text{O} + \text{OH} + \text{M}$	$\text{HO}_2 + \text{M}$	L
$\text{H} + \text{O}_2 + \text{M}$	$\text{HO}_2 + \text{M}$	M
$\text{OH} + \text{OH}$	H_2O_2	N
$\text{OH} + \text{OH} + \text{M}$	H_2O_2	O
$\text{O} + \text{O}_3$	$\text{O}_2 + \text{O}_2$	P
$\text{O}_3 + \text{H}$	$\text{O}_2 + \text{OH}$	Q
$\text{OH} + \text{CO}$	$\text{CO}_2 + \text{H}$	R
$\text{CO} + \text{O}$	CO_2	S
$\text{CO} + \text{O} + \text{M}$	$\text{CO}_2 + \text{M}$	T
$\text{CO} + \text{O}$	$\text{CO}_2 + h\nu$	U

Reactions P and Q were not considered because of the assumption of no O_3 in the exhaust.

Reaction S ($CO + O \rightleftharpoons CO_2$) was not considered since for CO , O and CO_2 in their ground states the reaction is spin forbidden¹². The possible reaction $CO + O_2 \rightleftharpoons CO_2 + O$ has not been considered because it has been shown that $CO - O_2$ reactions go very slowly¹³. The $CO - O_2$ reaction rate increases as the O_2 becomes wetter¹⁴. Hence, it is assumed that the CO disappears through the reaction $CO + OH \rightleftharpoons H + CO_2$ at the temperatures of interest here (1000 - 4000 °K)¹⁰.

Westenberg and Fristrom¹⁵ state that if the $CO - O_2$ reaction contributes appreciably to the energy of the system it is hard to explain the catalytic effects of H_2O or H_2 (through OH) on the $CO - O_2$ reaction. $CO - O_2$ mixtures are stable up to moderately high temperatures.

Carbon particles were considered not to be present in the exhaust burning region. Gaydon²¹ states that many pre-mixed flames show luminosity due to hot carbon particles under conditions in which carbon formation would not be expected. When the total number of oxygen atoms exceeds the total number of carbon atoms in a hot gas mixture, then under equilibrium conditions all the carbon present will be present as CO and CO_2 and there will be no free solid carbon.

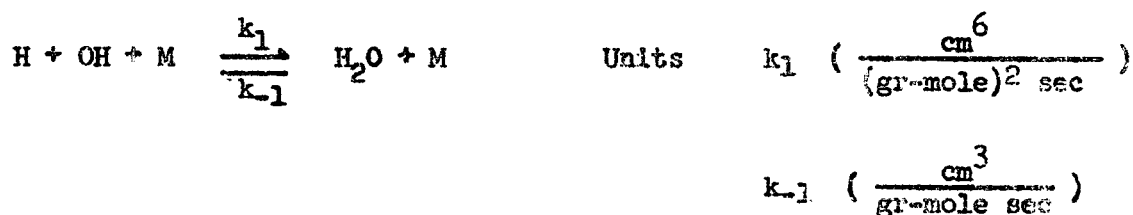
Hoglund, Carlson and Byron's²² work agrees with that of Gaydon. They report that energy is released by recombination of H atoms and OH radicals, by combustion of CO and H_2 molecules with O atoms

and O_2 molecules at high oxidizer to fuel ratios (greater than 2.), and by formation of solid carbon particles at low oxidizer to fuel ratios (less than 2.0). Since the oxidizer to fuel ratio considered here is 2.26 solid carbon was not considered.

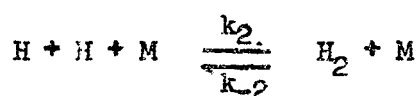
Appendix B Reaction Rates

The reaction rates found in the review of literature are listed.

The starred rate is the rate used in the analysis.



Reaction Rate	Temp. range °K	Reference
* $k_1 = 10^{23}/T^2$		(3)
$k_1 = 3 \times 10^{19}/T$		(3)
$k_{-1} = 2 \times 10^{22} T^{-3/2} e^{-114700/RT}$	1000 to 3500 (T in R°)	(27)
$k_1 = 7.5 \times 10^{19}/T$	1600 to 2800	(30)
$k_1 = 3.63 \times 10^{19}/T$	1000 to 4000	(31)
$k_1 = 4.5 \times 10^{21}/T^{1.5}$	1000 to 6000	(12)
$k_{-1} = 1.7 \times 10^{22}/T^{1.31}$	1000 to 6000	(12)



$$\text{Units } k_2 \left(\frac{\text{cm}^6}{(\text{gr-mole})^2 \text{ sec}} \right)$$

$$k_{-2} \left(\frac{\text{cm}^3}{\text{gr-mole sec}} \right)$$

Reaction Rate

Temp. range °K

Reference

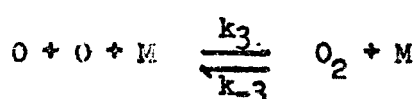
$$* k_2 = 5 \times 10^{21}/T^2 \quad (3)$$

$$k_2 = 2 \times 10^{18}/T \quad (3)$$

$$k_{-2} = 10^{21} T^{-1.5} e^{-103200/RT} \quad \begin{array}{l} 1000 \text{ to } 3500 \text{ } ^\circ\text{K} \\ (T \text{ in } R^\circ) \end{array} \quad (27)$$

$$k_2 = 3 \times 10^{18}/T \quad 1600 \text{ to } 2300 \quad (30)$$

$$k_2 = 3.267 \times 10^{18}/T \quad 1000 \text{ to } 4000 \quad (31)$$



$$\text{Units } k_3 \left(\frac{\text{cm}^6}{(\text{gr-mole})^2 \text{ sec}} \right)$$

$$k_{-3} \left(\frac{\text{cm}^3}{\text{gr-mole sec}} \right)$$

Reaction Rate

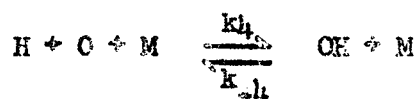
Temp. range °K

Reference

$$* k_3 = 2 \times 10^{18}/T \quad (3)$$

$$k_3 = 18.5 \times 10^{16}/T^{1.5} \quad \begin{array}{l} 1000 \text{ to } 3500 \text{ } ^\circ\text{K} \\ (T \text{ in } R^\circ) \end{array} \quad (27)$$

$$k_3 = 3.63 \times 10^{17}/T \quad 1000 \text{ to } 4000 \quad (31)$$



$$\text{Units } k_4 \left(\frac{\text{cm}^3}{(\text{gr-mole})^2 \text{ sec}} \right)$$

$$k_{-4} \left(\frac{\text{cm}^3}{(\text{gr-mole}) \text{ sec}} \right)$$

Reaction Rate

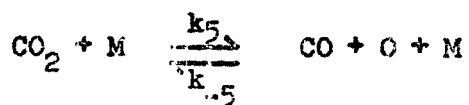
Temp. range °K

Reference

$$* k_4 = 2 \times 10^{18}/T \quad (3)$$

$$k_4 \approx 10^{15} - 10^{16} \quad 1600 \text{ to } 2800 \quad (30)$$

$$k_4 = 3.63 \times 10^{18}/T \quad 1000 \text{ to } 4000 \quad (31)$$



$$\text{Units } k_5 \left(\frac{\text{cm}^3}{\text{gr-mole sec}} \right)$$

$$k_{-5} \left(\frac{\text{cm}^3}{(\text{gr-mole})^2 \text{ sec}} \right)$$

Reaction Rate

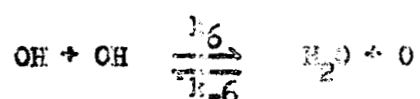
Temp. range °K

Reference

$$k_{-5} = 4 \times 10^{17} e^{-3500/RT} \quad (27)$$

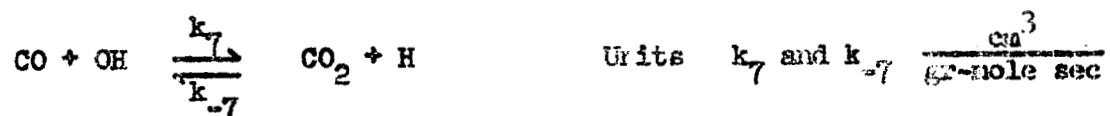
$$* k_5 = 3 \times 10^{11} T^{1/2} e^{-86000/RT} \quad (28)$$

$$k_{-5} = 1.82 \times 10^{19} e^{-4000/RT} \quad 1000 \text{ to } 4000 \quad (31)$$



Units k_6 and k_{-6} $\frac{\text{cm}^3}{\text{mole sec}}$

Reaction Rate	Temp. range °K	Reference
$k_6 = 10^{12.88} e^{-1000/RT}$	500 to 2000	(24)
$k_{-6} = 10^{13.92} e^{-1800/RT}$	300 to 2000	(24)
$k_{-6} = 5 \times 10^{14} e^{-1800/RT}$		(3)
* $k_6 = 3 \times 10^{14} e^{-3020/T}$	1000 to 3000	(1)
$k_6 = 6.025 \times 10^{12} e^{-1000/RT}$	1000 to 4000	(31)
$k_6 = 7.6 \times 10^{12} e^{-1000/RT}$	1000 to 6000	(12)
$k_{-6} = 6.9 \times 10^{13} e^{-17750/RT}$	1000 to 6000	(12)



Reaction Rate	Temp. range °K	Reference
$k_7 = 1.0 \times 10^{11.9}$	1650	(23)
$k_{-7} = 3 \times 10^{21} e^{-33000/RT}$		(25)
$k_7 = 5 \times 10^{12} e^{-6000/RT}$		(26)
* $k_7 = 10^{13} e^{-10000/RT}$		(3)
$k_7 = 5 \times 10^{12} e^{-7000/RT}$		(22)
$k_7 = 7.23 \times 10^{12} e^{-7700/RT}$	1000 to 4000	(31)
$k_7 = 3.2 \times 10^{12} e^{-6300/RT}$	1000 to 6000	(12)
$k_{-7} = 3 \times 10^{15} e^{-33000/RT}$	1200 to 1350	(31)



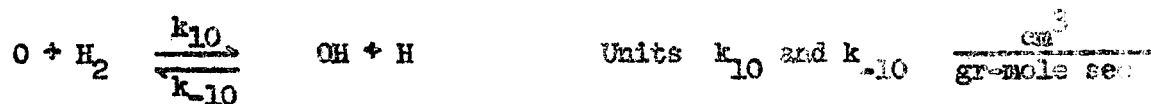
Units k_8 and k_{-8} $\frac{\text{cm}^3}{\text{gr-mole sec}}$

Reaction Rate	Temp. range °K	Reference
$k_8 = 10^{13.8} e^{-5900/RT}$	300 to 2000	(24)
$k_{-8} = 10^{14.48} e^{-21000/RT}$	300 to 2000	(24)
$k_{-8} = 10^{15} e^{-25000/RT}$		(3), (21)
* $k_8 = 3 \times 10^{14} e^{-3020/T}$	1000 to 3000	(1)
$k_8 = 3.0125 \times 10^{13} e^{-5500/RT}$	1000 to 4000	(31)
$k_8 = 6.3 \times 10^{13} e^{-5900/RT}$	1000 to 6000	(12)
$k_{-8} = 2.4 \times 10^{14} e^{-20700/RT}$	1000 to 6000	(12)
$k_8 = 10^{15} e^{-25500/RT}$	1000 to 6000	(32)



Units k_9 and k_{-9} $\frac{\text{cm}^3}{\text{gr-mole sec}}$

Reaction Rates	Temp. range °K	Reference
$k_9 = 1 \times 10^{14.78} e^{-1800/RT}$	1100 to 1500	(23)
$k_9 = 10^{14.86} e^{-16900/RT}$	1500 to 1700	(24)
$k_{-9} = 10^{13.75} e^{-1000/RT}$	300 to 2000	(24)
$k_9 = 4 \times 10^{14} e^{-18000/RT}$		(26)
* $k_9 = 5 \times 10^{14} e^{-18000/RT}$		(3), (22)
$k_9 = 3 \times 10^{14} e^{-8810/T}$		(1)
$k_9 = 1.989 \times 10^{14} e^{-16700/RT}$	1000 to 4000	(31)
$k_9 = 2.4 \times 10^{14} e^{-16750/RT}$		(12)
$k_{-9} = 3.2 \times 10^{11} T^{.47} e^{-100/RT}$		(12)



Reaction Rates	Temp. range °K	References
$k_{10} = 10^{12.4} e^{-7700/RT}$	300 to 2000	(24)
$k_{-10} = 10^{12.76} e^{-5800/RT}$	300 to 2000	(24)
$k_{10} = 1.2 \times 10^{13} e^{-9200/RT}$	1200 to 3500	(27)
$k_{10} = 3 \times 10^{14} e^{-4030/T}$	1000 to 3000	(1), (22)
* $k_{10} = 7 \times 10^{12} e^{-8500/RT}$		(3)
$k_{10} = 3.013 \times 10^{13} e^{-8300/RT}$	1000 to 4000	(31)
$k_{10} = 1.4 \times 10^{12} e^{-5190/RT}$		(12)
$k_{-10} = 6.9 \times 10^{13} e^{-17750/RT}$		(12)



Reaction Rates	Temp. range °K	References
$k_{11} = 1.8 \times 10^9 T^{\frac{1}{2}} e^{-3000/RT}$		(24)
* $k_{11} = 2 \times 10^{11} e^{-4500/RT}$		(29)
$k_{11} = 1 \times 10^{10} e^{-4000/RT}$		(29)

The Effect of Turbulence on Reaction Rates

To see how turbulence affects chemical kinetics, one must look at the rate constants. These rate constants have been obtained by theoretical and/or experimental means under the cited assumption that thermodynamic equilibrium roughly prevails and that non-equilibrium prevails only with respect to chemical composition. Consequently equipartition of energy among particles and internal degrees of freedom is assumed to exist, at least approximately. In high speed turbulent flow these assumptions are open to question. Therefore it may not be valid to use the classical chemical rate expressions as instantaneous rates. However, Ferri, Libby and Zakkay² state that the following statements can be made. At a fixed point in the flow, if the velocity squared fluctuations are significant with respect to $2 k T/m$, then these fluctuations significantly influence the collision processes. This appears to be the case for mixing processes of very high velocity streams having very small ratios of static to total enthalpy. In this case the enthalpy connected with the fluctuating process is of the same order as the static enthalpy. Consequently the number of a given type of collision and the mechanism of collisions could be quite different from the values given by statistical mechanics based on thermodynamic equilibrium.

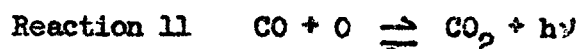
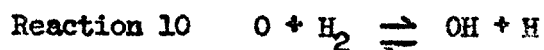
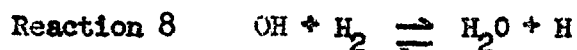
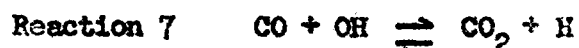
The effect of turbulence on collision mechanism can be looked at by considering a reaction following an Arrhenius law. Turbulence affects the temperature in the exponent of the expression and the function of temperature which multiplies the exponential. In two-body reactions the

reaction rate increases greatly with the relative velocity between the two colliding particles through the exponential of the rate constant on temperature ($k T \sim \frac{1}{2} v^2$) (see reactions listed above). Consequently a large fluctuation in the absolute velocity will increase the reaction rate for reactions following an Arrhenius law (two-body reactions). For three-body reactions, where the rate constant does not have an exponential term, it is expected that turbulence affects the reaction rates by increasing the probability of collisions. The above implies that the two-body reactions would be accelerated more than the three-body reactions by turbulence.

Appendix C Reaction EnergiesUnits kilocal/(cm³ sec)

Negative number implies energy release

Reaction 2 (x 10 ⁵)	Reaction 7 (x 10 ²)	Reaction 8	Reaction 10 (x 10 ⁴)	Reaction 11 (x 10 ³)	T °K	ρ
46	- 10	- 5	9	- 8	1438	.3
61	- 12	- 6	13	- 12	1497	.4
80	- 15	- 8	19	- 16	1511	.5
136	- 20	- 10	32	- 27	1539	.6
226	- 26	- 12	51	- 42	1567	.7
367	- 33	- 15	82	- 65	1595	.8
339	- 31	- 15	84	- 67	1595	.9
230	- 25	- 12	70	- 57	1581	1.0
86	- 14	- 7	39	- 33	1539	1.1
15	- 5	- 3	12	- 11	1469	1.2
2	- 2	- 1	3	- 4	1400	1.3
.1	- .5	- .3	.5	- .6	1302	1.4
.004	- .09	- .06	.05	- .06	1190	1.5
0	- .009	- .008	.002	- .003	1078	1.6
0	0	0	0	0	938	1.7
0	0	0	0	0	812	1.8



Reactions 1, 3, and 4 were assumed to be in equilibrium, reaction 5 was 1000 times less energetic than reaction 2, and reactions 6 and 9 were found to be in equilibrium; therefore these reactions are not listed.

Appendix D Discussion of the Carbon Monoxide - Oxygen Reaction

The carbon monoxide - oxygen reaction is a radiation producing reaction. (See Reaction U of Appendix A, Table A-I.) The continuum and flame band radiation are also observed in hydrocarbon - air flames, but are most intense in carbon - oxygen flames¹⁶.

In explosions at (initially) 100 to 200 mm Hg pressure, it is estimated that the continuum represents about 90 % of the radiated energy. The intensity of the flame bands relative to the continuum has been reported to increase with decreasing pressure and temperature. In fact, Clyne and Thrush¹⁷ found at temperatures between 200 and 300 °K and very low pressure that the C - CO system emits flame bands and no continuum.

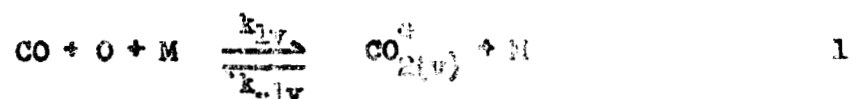
Kaskan¹⁶ noted no marked change in the ratio of continuum to flame band radiation with change in temperature, or pressure from .158 to 1 atmosphere pressure, although there seemed to be a slight strengthening of the flame bands relative to the continuum at the lower pressures. The ultra-violet end of the spectrum was strengthened with increasing temperature. In general, Kaskan¹⁶ found that all the spectra had the same spectral distribution above 4200 Å and that the spectrum was noticeable strengthened below 4200 Å.

The maximum intensity of the CO - O system emission occurs at about 4000 Å. Clyne and Thrush¹⁷ concluded that a similar mechanism controls the radiation in the visible and ultra-violet parts of the

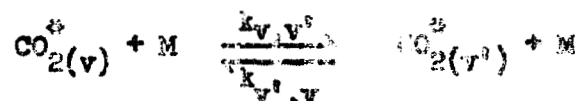
spectrum. They state that the continuum probably consists of extended unresolved rotational structure of the flame bands and the continuum arises from an overlapping of the rotational structure.

In the $\text{CO} - \text{O}$ chemiluminescent combination reaction the steady state of any vibrational level v of the excited electronic state of the molecule is controlled by the rates of the following processes.

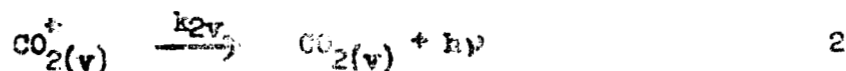
(i) Stabilization and redissociation



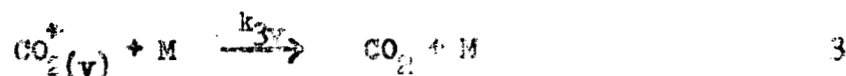
(ii) Vibrational energy transfer



(iii) Radiation



(iv) Collisional electronic quenching



Assuming that 1 and 3 are rapid compared with the time scale of the system the steady state approximation can be applied to the population of one vibrational level of CO_2^+ .

$$\begin{aligned} \frac{d [\text{CO}_2^+] (v)}{dt} = 0 = & k_{1v} [\text{CO}] [\text{O}] [\text{M}] - k_{-1v} [\text{CO}_2^+] (v) [\text{M}] \\ & + \sum_{v'} k_{v',v} [\text{CO}_2^+] (v') [\text{M}] - \sum_{v'} k_{v,v'} [\text{CO}_2^+] (v) [\text{M}] \end{aligned}$$

$$- k_{2v} [\text{CO}_2^*]_{(v)} - k_3 [\text{M}] [\text{CO}_2^*]_{(v)} \quad 4$$

and the total emission is given by

$$I = \sum_v k_{2v} [\text{CO}_2^*]_{(v)} \quad 5a$$

$$= \sum_v k_{2v} \left[\frac{[\text{M}] \left[k_{1v} [\text{CO}] [\text{O}] + \sum_{v'} k_{v',v} [\text{CO}_2^*]_{(v')} \right]}{k_{2v} + [\text{M}] (k_{1v} + k_{3v} + \sum_{v'} k_{v',v})} \right] \quad 5b$$

the total rate of recombination by the excited state is

$$\frac{d [\text{CO}_2^*]_{(v)}}{dt} = \sum_v (k_{2v} + k_{3v} [\text{M}]) [\text{CO}_2^*]_{(v)} \quad 6$$

If the quenching step 3 is much faster than the emitting step 2, which is a likely possibility, the emission is reduced¹², $k_{3v}[\text{M}] \gg k_{2v}$ and the expression for intensity 5b becomes

$$I = \sum_v k_{2v} \frac{(k_{1v} [\text{CO}] [\text{O}] + \sum_{v'} k_{v',v} [\text{CO}_2^*]_{(v')})}{(k_{1v} + k_{3v} + \sum_{v'} k_{v',v})} \quad 7$$

If the range of frequencies involved in the emission process 2 is not too large compared with the mean frequency emitted, it can be assumed that k_{2v} and k_{3v} are independent of v and hence equations 5a and 6 combine to give

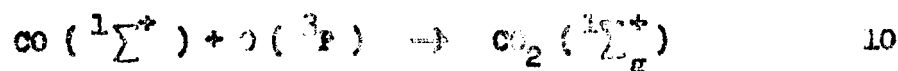
$$\frac{d [\text{CO}_2^*]}{dt} = \frac{k_{2v} + k_{3v} [\text{M}]}{k_{2v}} I = \frac{(k_2 + k_3 [\text{M}])}{k_2} I_0 [\text{CO}] [\text{O}] \quad 8$$

since¹⁸,

$$I = I_0 [CO] [O] \quad 9$$

Kashan and Browne¹² give a value of $2.0 \times 10^5 \exp(-2200/RT) \frac{\text{cm}^3}{\text{gr-atom}} \text{ sec}$ for I_0 .

The overall combination reaction



is spin forbidden, and the spin reversal occurs either

- (i) in the stabilization of an excited CO_2 molecule by a third body,
- (ii) in a radiationless transition of an excited CO_2 molecule before or after radiation, or
- (iii) in the radiative process.

In case (i) oxygen, with a triplet ground state $^3\Sigma_g^-$ would increase the intensity by facilitating spin reversal. In case (iii) the intensity would be expected to decrease since the rate of quenching k_3 of the triplet CO_2 molecules would be accelerated relative to the rate of emission k_2 . Clyne and Thrush¹⁷ conclude that spin reversal occurs in the radiationless transition between two electronic states of CO (ii). This transition would occur either before or after the emission process. The latter case implies a very low-lying triplet state for CO_2 . No low-lying triplet (or singlet) state of CO_2 has been detected spectroscopically, nor are any to be expected from molecular orbital considerations. Clyne and Thrush therefore conclude that the CO flame band emission is

mainly a singlet-singlet transition to the ground state of CO_2 and that spin reversal occurs in a radiationless transition between two excited states of CO_2 .

The situation involving the direct combination of CO and O by reactions S and T is somewhat confused at the present time. Flame work, which has been done under conditions where CO and O may co-exist in appreciable concentrations, has not shed any light on this matter of direct recombination¹².

The evidence on reactions S and T should be further considered in the light of information on the radiation producing reaction U. The blue light from CO containing flames consists of a wide band of emission from about 3000 \AA to 6500 \AA and appears as a continuum underlied with a weak complex band system. It appears quite likely that only one process is involved in continuum and band system and that the continuum is merely the result of high temperature smearing of the bands¹².

Appendix E Transformation of the Compressible Mixing Layer

Nomenclature

g	=	Scaling function - to align $Y = 0$ with dividing streamline
h	=	Static enthalpy
h^0	=	Stagnation enthalpy
H^0	=	Stagnation enthalpy flux per unit width
I	=	Momentum flux per unit width
m	=	Mass flux per unit width
P	=	Static pressure in flow
q	=	Heat flux
u	=	Velocity in streamwise direction in physical plane
v	=	Normal velocity in physical plane
V	=	Normal velocity in transformed plane = $v + u g'$
x	=	Distance in streamwise direction
y	=	Normal distance in physical plane
Y	=	Normal distance in transformed plane = $y + g(x)$
δ	=	Boundary layer thickness
δ^*	=	Displacement thickness
θ	=	Momentum thickness
ϕ	=	Stagnation enthalpy thickness
σ	=	Transformation variable
η	=	Transformation variable
ξ	=	Transformation variable
ρ	=	Density of the flow
τ	=	Shear stress
μ	=	Coefficient of viscosity
ψ	=	Streamfunction
ϵ	=	Eddy viscosity

Subscripts

1	=	Freestream lower condition
2	=	Freestream upper condition
U	=	Upper region
L	=	Lower region

Consider the boundary layer equations for two-dimensional compressible flow.

$$\text{Continuity:} \quad \frac{\partial}{\partial x} (\rho u) + \frac{\partial}{\partial y} (\rho v) = 0 \quad (1)$$

$$\text{Momentum:} \quad \rho u \frac{\partial u}{\partial x} + \rho v \frac{\partial u}{\partial y} = - \frac{\partial p}{\partial x} + \frac{\partial \tau}{\partial y} \quad (2)$$

$$\text{Energy:} \quad \rho u \frac{\partial h^0}{\partial x} + \rho v \frac{\partial h^0}{\partial y} = \frac{\partial q}{\partial y} + u \frac{\partial \tau}{\partial y} \quad (3)$$

After transforming the variables to V and Y , one can eliminate V by use of the continuity equation and integrate the momentum and energy equations from $-\infty$ to ∞ .

$$\begin{aligned} \int_{-\infty}^{\infty} \frac{\partial}{\partial x} (\rho u^2) dx &= u_2 \int_0^{\infty} \frac{\partial}{\partial x} (\rho u) dY - u_1 \int_0^{\infty} \frac{\partial}{\partial x} (\rho u) dY \\ &\quad - (\delta_2 + \delta_1) \frac{dp}{dx} \end{aligned} \quad (4)$$

$$\int_{-\infty}^{\infty} \frac{\partial}{\partial x} (\rho u h^0) dY = h^0_2 \int_0^{\infty} \frac{\partial}{\partial x} (\rho u) dY - h^0_1 \int_0^{\infty} \frac{\partial}{\partial x} (\rho u) dY \quad (5)$$

It is now convenient to define the mass, momentum, and stagnation enthalpy flux per unit width for the upper and lower region as:

$$m = \int_{-\infty}^{\infty} \rho u dY \quad (4a) \quad I = \int_{-\infty}^{\infty} \rho u^2 dY \quad (5a) \quad H^0 = \int_{-\infty}^{\infty} \rho u h^0 dY \quad (6a)$$

$$m_U = \int_0^{\infty} \rho u dY \quad (4b) \quad I_U = \int_0^{\infty} \rho u^2 dY \quad (5b) \quad H^0_U = \int_0^{\infty} \rho u h^0 dY \quad (6b)$$

$$m_L = \int_{-\infty}^0 \rho u dY \quad (4c) \quad I_L = \int_{-\infty}^0 \rho u^2 dY \quad (5c) \quad H^0_L = \int_{-\infty}^0 \rho u h^0 dY \quad (6c)$$

$$m = m_U + m_L \quad I = I_U + I_L \quad H^0 = H^0_U + H^0_L$$

The equations become

$$\frac{dI_U}{dx} + \frac{dI_L}{dx} + (\delta_2 + \delta_1) \frac{dP}{dx} = u_2 \frac{dm_U}{dx} + u_1 \frac{dm_L}{dx} \quad (7a)$$

$$\frac{dH^0_U}{dx} + \frac{dH^0_L}{dx} = h_2^0 \frac{dm_U}{dx} + h_1^0 \frac{dm_L}{dx} \quad (7b)$$

One can now define the displacement, momentum, and stagnation enthalpy thicknesses for each region as:

$$\delta_U^* = \int_0^\infty \left(1 - \frac{\rho u}{\rho_2 u_2}\right) dy \quad (8a) \quad \theta_U = \int_0^\infty \frac{\rho u}{\rho_2 u_2} \left(1 - \frac{u}{u_2}\right) dy \quad (9a)$$

$$\delta_L^* = \int_{-\infty}^0 \left(1 - \frac{\rho u}{\rho_1 u_1}\right) dy \quad (8b) \quad \theta_L = \int_{-\infty}^0 \frac{\rho u}{\rho_1 u_1} \left(1 - \frac{u}{u_1}\right) dy \quad (9b)$$

$$\phi_U = \int_0^\infty \frac{\rho u}{\rho_2 u_2} \left(1 - \frac{h^0}{h_2^0}\right) dy \quad (10a)$$

$$\phi_L = \int_{-\infty}^0 \frac{\rho u}{\rho_1 u_1} \left(1 - \frac{h^0}{h_1^0}\right) dy \quad (10b)$$

Making use of these definitions the final form of the compressible equations is (assuming $h_2^0 = \text{constant}$ and $h_1^0 = \text{constant}$)

$$\frac{d}{dx} \left\{ \rho_2 u_2^2 \theta_U + \rho_1 u_1^2 \theta_L \right\} - (\delta_U^* + \delta_L^*) \frac{dP}{dx} = 0 \quad (11a)$$

$$\frac{d}{dx} \left\{ \rho_2 u_2 h_2^0 \phi_U + \rho_1 u_1 h_1^0 \phi_L \right\} = 0 \quad (11b)$$

Now one must consider an unspecified low speed fluid. As Coles and Crocco did, denote the corresponding quantities and equations with a bar as below

$$\bar{m} = \int_{-\infty}^{\infty} \bar{\rho} \bar{u} d\bar{y} \quad (4a) \quad \bar{I} = \int_{-\infty}^{\infty} \bar{\rho} \bar{u}^2 d\bar{y} \quad (5a) \quad \bar{H} = \int_{-\infty}^{\infty} \bar{\rho} \bar{u} \bar{h} d\bar{y} \quad (6a)$$

$$\bar{m}_U = \int_{\sigma}^{\infty} \bar{\rho} \bar{u} d\bar{y} \quad (4b) \quad \bar{I}_U = \int_{\sigma}^{\infty} \bar{\rho} \bar{u}^2 d\bar{y} \quad (5b) \quad \bar{H}_U = \int_{\sigma}^{\infty} \bar{\rho} \bar{u} \bar{h} d\bar{y} \quad (6b)$$

$$\bar{m}_L = \int_{-\infty}^{\sigma} \bar{\rho} \bar{u} d\bar{y} \quad (4c) \quad \bar{I}_L = \int_{-\infty}^{\sigma} \bar{\rho} \bar{u}^2 d\bar{y} \quad (5c) \quad \bar{H}_L = \int_{-\infty}^{\sigma} \bar{\rho} \bar{u} \bar{h} d\bar{y} \quad (6c)$$

$$\bar{J}_U^* = \int_{\sigma}^{\infty} \left(1 - \frac{\bar{\rho} \bar{u}}{\bar{\rho}_2 \bar{u}_2}\right) d\bar{y} \quad (8a) \quad \bar{\Theta}_U = \int_{\sigma}^{\infty} \frac{\bar{\rho} \bar{u}}{\bar{\rho}_2 \bar{u}_2} \left(1 - \frac{\bar{u}}{\bar{u}_2}\right) d\bar{y} \quad (9a)$$

$$\bar{J}_L^* = \int_{-\infty}^{\sigma} \left(1 - \frac{\bar{\rho} \bar{u}}{\bar{\rho}_1 \bar{u}_1}\right) d\bar{y} \quad (8b) \quad \bar{\Theta}_L = \int_{-\infty}^{\sigma} \frac{\bar{\rho} \bar{u}}{\bar{\rho}_1 \bar{u}_1} \left(1 - \frac{\bar{u}}{\bar{u}_1}\right) d\bar{y} \quad (9b)$$

$$\bar{\Phi}_U = \int_{\sigma}^{\infty} \frac{\bar{\rho} \bar{u}}{\bar{\rho}_2 \bar{u}_2} \left(1 - \frac{\bar{h}}{\bar{h}_2}\right) d\bar{y} \quad (10a)$$

$$\bar{\Phi}_L = \int_{-\infty}^{\sigma} \frac{\bar{\rho} \bar{u}}{\bar{\rho}_1 \bar{u}_1} \left(1 - \frac{\bar{h}}{\bar{h}_1}\right) d\bar{y} \quad (10b)$$

$$\text{Momentum: } \frac{d}{dx} \left\{ \bar{\rho}_2 \bar{u}_2^2 \bar{\Theta}_U + \bar{\rho}_1 \bar{u}_1^2 \bar{\Theta}_L \right\} = (\bar{J}_U^* + \bar{J}_L^*) \frac{d\bar{P}}{dx} \quad (11a)$$

$$\text{Energy: } \frac{d}{dx} \left\{ \bar{\rho}_2 \bar{u}_2 \bar{h}_2 \bar{\Phi}_U + \bar{\rho}_1 \bar{u}_1 \bar{h}_1 \bar{\Phi}_L \right\} = 0 \quad (11b)$$

(assuming $\bar{h}_1 = \text{constant}$ and $\bar{h}_2 = \text{constant}$)

The stagnation enthalpy has been replaced by the static enthalpy for the low speed flow.

Now one must find a transformation which when applied to equations (11a) and (11b) will give equations (11a) and (11b) respectively. By introducing the stream functions ψ and $\bar{\psi}$ in the usual way

$$\psi = \int_0^Y \rho u \, dY' \quad (12)$$

$$\bar{\psi} = \int_0^{\bar{Y}} \bar{\rho} \bar{u} \, d\bar{Y}' \quad (13)$$

It is possible to define the following transformation

$$\sigma(x) = \frac{\bar{\psi}}{\psi} \quad (14a) \quad \eta(x) = \frac{\bar{\rho}}{\rho} \frac{d\bar{Y}}{dY} \quad \frac{dx}{dx} = 1 \quad (14b) \quad (14c)$$

By substituting equations (14a) - (14c) into equations 4 - 10 and comparing with equations 4 - 10, it is easily shown that the following relations are true.

$$\bar{m}_U = \sigma m_U \quad (15a)$$

$$\bar{m}_L = \sigma m_L \quad (15b)$$

$$\bar{I}_U = \frac{\sigma^2}{\eta} I_U \quad (16a)$$

$$\bar{I}_L = \frac{\sigma^2}{\eta} I_L \quad (16b)$$

$$\bar{H}_U = \sigma \frac{\bar{h}_2}{h_2^0} H_U \quad (17a)$$

$$\bar{H}_L = \sigma \frac{\bar{h}_1}{h_1^0} H_L \quad (17b)$$

$$\bar{\delta}_U^* = \eta \frac{\rho_2}{\bar{\rho}_2} \left\{ \delta_U^* - \int_0^\infty \left(1 - \frac{\bar{\rho}_2 \rho}{\bar{\rho} \rho_2} \right) dy \right\} \quad (18a)$$

$$\bar{\delta}_L^* = \eta \frac{\rho_1}{\bar{\rho}_1} \left\{ \delta_L^* - \int_{-\infty}^0 \left(1 - \frac{\bar{\rho}_1 \rho}{\bar{\rho} \rho_1} \right) dy \right\} \quad (18b)$$

$$\bar{\theta}_U = \eta \frac{\rho_2}{\bar{\rho}_2} \theta_U \quad (19a)$$

$$\bar{\theta}_L = \eta \frac{\rho_1}{\bar{\rho}_1} \theta_L \quad (19b)$$

$$\bar{\theta}_U = \eta \frac{\rho_2}{\bar{\rho}_2} \phi_U \quad (20a) \quad \text{if} \quad \frac{\bar{h}}{\bar{h}_2} = \frac{h^0}{h_2^0} \quad (21a)$$

$$\bar{\theta}_L = \eta \frac{\rho_1}{\bar{\rho}_1} \phi_L \quad (20b) \quad \text{if} \quad \frac{\bar{h}}{\bar{h}_1} = \frac{h^0}{h_1^0} \quad (21b)$$

$$\frac{d\bar{P}}{d\bar{x}} = \frac{\sigma^2}{\eta^2} \frac{\bar{\rho}_2}{\rho_2} \left\{ \frac{dP}{dx} + \rho_2 u_2^2 \frac{d}{dx} \left(\ln \frac{h}{\sigma} \right) \right\} \quad (22a)$$

$$= \frac{\sigma^2}{\eta^2} \frac{\bar{\rho}_1}{\rho_1} \left\{ \frac{dP}{dx} + \rho_1 u_1^2 \frac{d}{dx} \left(\ln \frac{h}{\sigma} \right) \right\} \quad (22b)$$

Equations (21a) and (21b) imply that $\bar{h}_2/h_2^0 = \bar{h}_1/h_1^0$

Substituting the appropriate expressions into equation (11a) and comparing with equation (11a) yields

$$\begin{aligned}
 0 = & \frac{dP}{dx} \left[\int_0^\infty \left(1 - \frac{\bar{\rho}_2 \rho}{\bar{\rho} \rho_2} \right) dy + \int_{-\infty}^0 \left(1 - \frac{\bar{\rho}_1 \rho}{\bar{\rho} \rho_1} \right) dy \right] \\
 & + \frac{d}{dx} \ln \frac{h}{\sigma} \left[\rho_2 u_2^2 (-s_U^* - \phi_U + \int_0^\infty \left(1 - \frac{\bar{\rho}_2 \rho}{\bar{\rho} \rho_2} \right) dy) \right. \\
 & \left. + \rho_1 u_1^2 (-s_L^* - \phi_L + \int_{-\infty}^0 \left(1 - \frac{\bar{\rho}_1 \rho}{\bar{\rho} \rho_1} \right) dy) \right] \\
 & + \frac{d}{dx} \ln \sigma (\rho_2 u_2^2 \phi_U + \rho_1 u_1^2 \phi_L)
 \end{aligned} \tag{23a}$$

This equation can be greatly simplified. Assuming a perfect polytropic gas such that

$$\begin{aligned}
 \frac{\bar{\rho}_2}{\bar{\rho}} &= \frac{\bar{h}}{\bar{h}_2} = \frac{h^0}{h_2^0} & \frac{\bar{\rho}_1}{\bar{\rho}} &= \frac{\bar{h}}{\bar{h}_1} = \frac{h^0}{h_1^0} \\
 \frac{\rho_2}{\rho} &= \frac{h}{h_2} & \frac{\rho_1}{\rho} &= \frac{h}{h_1}
 \end{aligned} \tag{24a}$$

then

$$\begin{aligned}
 \int_0^\infty \left(1 - \frac{\bar{\rho}_2 \rho}{\bar{\rho} \rho_2} \right) dy &= \frac{u_2^2}{2 h_2^0} (s_U^* + \phi_U) \\
 \int_{-\infty}^0 \left(1 - \frac{\bar{\rho}_1 \rho}{\bar{\rho} \rho_1} \right) dy &= \frac{u_1^2}{2 h_1^0} (s_L^* + \phi_L)
 \end{aligned}$$

and

$$\mathcal{F}_U^* = h \frac{\rho_2}{\rho_2} \left[\mathcal{F}_U^* \left(1 - \frac{u_2^2}{2 h_2^0} \right) - \frac{u_2^2}{2 h_2^0} \phi_U \right] \quad (24b)$$

$$\mathcal{F}_L^* = h \frac{\rho_1}{\rho_1} \left[\mathcal{F}_L^* \left(1 - \frac{u_1^2}{2 h_1^0} \right) - \frac{u_1^2}{2 h_1^0} \phi_L \right] \quad (24c)$$

after substituting and noting that

$$\mathcal{F}_U^* + \phi_U - \frac{u_2^2}{2 h_2^0} (\mathcal{F}_U^* + \phi_U) = \frac{h_2}{h_2^0} (\mathcal{F}_U^* + \phi_U) \quad (24d)$$

$$\mathcal{F}_L^* + \phi_L - \frac{u_1^2}{2 h_1^0} (\mathcal{F}_L^* + \phi_L) = \frac{h_1}{h_1^0} (\mathcal{F}_L^* + \phi_L) \quad (24e)$$

$$\frac{dP}{dx} \frac{u_2^2}{2 h_2^0} (\mathcal{F}_U^* + \phi_U) = \rho_2 u_2^2 \left[\frac{1}{2 h_2^0} \frac{dh_2}{dx} (\mathcal{F}_U^* + \phi_U) \right] \quad (24f)$$

$$\frac{dP}{dx} \frac{u_1^2}{2 h_1^0} (\mathcal{F}_L^* + \phi_L) = \rho_1 u_1^2 \left[\frac{1}{2 h_1^0} \frac{dh_1}{dx} (\mathcal{F}_L^* + \phi_L) \right] \quad (24g)$$

one can obtain

$$\begin{aligned} & \rho_2 u_2^2 \left\{ \phi_U \frac{d}{dx} \ln \sigma - \frac{h_2}{h_2^0} (\mathcal{F}_U^* + \phi_U) \frac{d}{dx} \ln \left[\frac{h}{\sigma} \left(\frac{h_2^0}{h_2} \right)^{\frac{1}{2}} \right] \right\} \\ & + \rho_1 u_1^2 \left\{ \phi_L \frac{d}{dx} \ln \sigma - \frac{h_1}{h_1^0} (\mathcal{F}_L^* + \phi_L) \frac{d}{dx} \ln \left[\frac{h}{\sigma} \left(\frac{h_1^0}{h_1} \right)^{\frac{1}{2}} \right] \right\} = 0 \end{aligned} \quad (23b)$$

For a given $\sigma(x)$, equation (23b) can be integrated for $\frac{h}{\sigma}$ and consequently can be solved for $h(x)$.

In like manner one can substitute the appropriate relations into equation (11b) and in comparison with equation (11b) finds

$$(\rho_2 u_2 h_2^0 \phi_U + \rho_1 u_1 h_1^0 \phi_L) \frac{d}{dx} \left(\sigma \frac{\bar{h}}{h^0} \right) = 0 \quad (25)$$

This equation implies that is $\left(\sigma \frac{\bar{h}}{h^0} \right)$ is not equal to a constant, then

$$\phi_U = - \frac{\rho_1 u_1 h_1^0}{\rho_2 u_2 h_2^0} \phi_L$$

So an immediate restriction must be imposed on the problem if σ is a function of the streamwise coordinate.

Consider the transformation of the momentum equation for zero pressure gradient. The resulting equation is

$$(\rho_2 u_2^2 \theta_U + \rho_1 u_1^2 \theta_L) \frac{d}{dx} \left(\frac{\sigma^2}{h} \right) = 0 \quad (26)$$

If the boundary layer growth on the plate separating the two flows initially is neglected, then $\theta_U(0)$ and $\theta_L(0)$ are both zero and $\rho_2 u_2^2 \theta_U + \rho_1 u_1^2 \theta_L$ can be equal to zero. However, this equation implies that

$$\theta_U = - \frac{(\rho_1 u_1^2)}{(\rho_2 u_2^2)} \theta_L$$

and places an additional restriction on the problem. If the initial boundary layer growth is not neglected, then neither $\theta_U(0)$ nor $\theta_L(0)$

are zero. Consequently equation (26) shows that $\sigma (\sigma/\eta)$ is equal to a constant. For zero pressure gradient, equation (22) implies that σ/η is a constant. Thus σ must be a constant, and η must be a constant.